Arabidopsis U1 snRNP subunit LUC7 functions in alternative splicing and preferential removal of terminal introns

Marcella de Francisco Amorim[1,2,3], Eva-Maria Willing[4], Emese Xochitl Szabo[1,2,3,*], Irina Droste-Borel[5], Boris Maček[5], Korbinian Schneeberger[4] and Sascha Laubinger[1,2,3,*]

[1] Centre for Plant Molecular Biology (ZMBP), University of Tuebingen, Tuebingen, Germany

[2] Chemical Genomics Centre (CGC) of the Max Planck Society, Dortmund, Germany

[3] Max Planck Institute for Developmental Biology, Tuebingen, Germany

[4] Max Planck Institute for Plant Breeding Research (MPIPZ), Cologne, Germany

[5] Proteome Centre, University of Tuebingen, Tuebingen, Germany

* present address: Carl von Ossietzky University, Oldenburg, Germany

Corresponding author: Sascha Laubinger (sascha.laubinger@uol.de)

Keywords: U1 snRNP, Splicing, Non-sense mediated mRNA decay (NMD), Polyadenylation, RNA transport, Arabidopsis

Abstract

Introns are removed by the spliceosome, a large complex composed of five ribonucleoprotein subcomplexes (U snRNP). The U1 snRNP, which binds to 5' splice sites, plays an essential role in early steps of the splicing reaction. Here, we show that Arabidopsis LUC7 is a U1 snRNP subunit that affects constitutive and alternative splicing. Interestingly, LUC7 specifically promotes splicing of a subset of terminal introns. Splicing of LUC7-dependent terminal introns is a prerequisite for nuclear export and can be modulated by stress. Globally, intron retention under stress conditions occurs preferentially among first and terminal introns, uncovering an unknown bias for splicing regulation in Arabidopsis. Taken together, our study reveals that the Arabidopsis U1 snRNP component LUC7 is important for alternative splicing and removal of terminal introns and it suggests that Arabidopsis terminal introns fine-tune gene expression under stress conditions.

37 # Introduction

38 Eukaryotic genes are often interrupted by non-coding sequences called introns that
39 are removed from pre-mRNAs while the remaining sequence, the exons, are joined
40 together. This process, called splicing, is an essential step before the translation of
41 the mature mRNAs and it offers a wide range of advantages for eukaryotic
42 organisms. For instance, alternative splicing allows the production of more than one
43 isoform from a single gene expanding the genome coding capacity (Kornblihtt *et al.*,
44 2013; Reddy *et al.*, 2013). In plants, alternative splicing contributes to essentially all
45 aspects of development and stress responses (Carvalho *et al.*, 2013; Staiger &
46 Brown, 2013). Alternative splicing can also generate transcripts with premature
47 termination codons (PTC) or/and a long 3'UTR, which may lead to RNA degradation
48 via the nonsense-mediated decay (NMD) pathway (Drechsel *et al.*, 2013; Kalyna *et*
49 *al.*, 2012; Shaul, 2015). Furthermore, splicing is coupled with other RNA processing
50 events, such as 3'end formation and RNA transport to the cytosol (Kaida, 2016;
51 Muller-McNicoll *et al.*, 2016).

52 Intron removal is catalyzed by a large macromolecular complex, the
53 spliceosome, which is formed by five small ribonucleoprotein particles (snRNP): the
54 U1, U2, U4, U5 and U6 snRNP. Each U snRNP contains a heteroheptameric ring of
55 Sm or Lsm proteins, snRNP-specific proteins and a uridine-rich snRNA. Additional
56 non-core spliceosomal proteins participate also during the splicing reaction affecting
57 exon-intron recognition/definition and thus splicing efficiency. The canonical splicing
58 cycle starts with binding of the U1 snRNP to the 5' splice site (5'ss), followed by
59 association of auxiliary proteins such as U2AF to the pre-mRNA, which facilitate the
60 recognition of the 3' splice site (3'ss). The thereby formed complex E recruits the U2
61 snRNP to generate complex A. In the next step, a trimeric complex consisting of
62 U4/U5/U6 snRNPs joins to form complex B. Several rearrangements and ejection of

63 the U1 and U4 snRNP are necessary to generate a catalytically active splicing
64 complex (Wahl *et al.*, 2009; Will & Luhrmann, 2011).

65 The fact that U1 snRNP is recruited to the 5'ss in the initial step of splicing
66 suggests that this complex is necessary for correct splicing site selection. Indeed, it
67 has been shown that U1-deficient zebrafish mutants accumulate alternative spliced
68 transcripts, suggesting that the U1 snRNP fulfills regulatory roles in splice site
69 selection (Rosel *et al.*, 2011). Although the spliceosome consists of stoichiometrically
70 equal amounts of each subunit, the U1 snRNP is more abundant than all the other
71 spliceosomal subcomplexes (Kaida, 2016; Kaida *et al.*, 2010). One reason for this is
72 that the U1 snRNP executes splicing independent functions. For instance, metazoan
73 U1 snRNP binds not only to the 5'ss, but also throughout the nascent transcript to
74 block a premature cleavage and polyadenylation (Berg *et al.*, 2012; Kaida *et al.*,
75 2010). Furthermore, the U1 snRNP is also important to regulate promoter
76 directionality and transcription (Almada *et al.*, 2013; Guiro & O'Reilly, 2015).

77 U1 snRNP complexes were purified and characterized from yeast and human.
78 The U1 snRNP contains the U1 snRNA, Sm proteins, three U1 core proteins (U1-
79 70K, U1-A and U1-C) and U1-specific accessory proteins, such as LUC7, PRP39
80 and PRP40. All these proteins are conserved in plants suggesting a U1 snRNP
81 composition very similar to that of yeast and metazoans (Koncz *et al.*, 2012; Reddy
82 *et al.*, 2013; Wang & Brendel, 2004). Interaction studies revealed that the U1 snRNP
83 associates with serine-arginine (SR) proteins, indicating that the complex
84 mechanisms for splicing site selection involve also non-snRNP proteins (Cho *et al.*,
85 2011; Golovkin & Reddy, 1998).

86 The function of the plant U1 snRNP is not well characterized. This might be
87 due to the fact that in *Arabidopsis thaliana*, *U1-70K*, *U1-A* and *U1-C* are single copy
88 genes and a complete knockout will probably cause lethality. On the other hand,

89 proteins such as PRP39, PRP40 and LUC7 come as small gene families, which will
90 require the generation of multiple mutants for functional studies. Other factors, such
91 as GEMIN2 or SRD2 are required for the functionality of all snRNPs, but not
92 specifically for U1 function (Ohtani & Sugiyama, 2005; Schlaen *et al.*, 2015). Only a
93 single U1 snRNP-specific gene, the *PRP39a* was characterized. *prp39a* mutants
94 flower late due to increased expression of the flowering time regulator *FLOWERING*
95 *LOCUS C* (*FLC*), but the mutant does not exhibit any additional developmental
96 defects (Wang *et al.*, 2007). In a reverse genetic approach, *U1-70K* expression was
97 specifically reduced in flowers by an antisense RNA and the resulting transgenic
98 plants exhibit strong floral defects (Golovkin & Reddy, 2003). Despite evidences that
99 U1 snRNP is essential for plant development, the functions of the U1 snRNP in
100 regulating the transcriptome of plants are unknown.

101 Here, we report on the functional characterization of an *Arabidopsis* mutant
102 impaired in U1 snRNP function. For this, we focused in this study on the U1 snRNP
103 component LUC7, which we show to be essential for normal plant development. Our
104 whole transcriptome analyses on *luc7* triple mutant show that impairments of LUC7s
105 affect constitutive and alternative splicing. Surprisingly, our results reveal the
106 existence of transcripts, in which terminal introns are preferentially retained in a
107 LUC7-dependent manner and that these unspliced terminal introns cause a nuclear
108 retention of the pre-mRNAs. Our findings are accompanied by the observation that
109 splicing of first and last introns is preferentially regulated under stress conditions. Our
110 results suggests that the plant U1 snRNP component LUC7 carries out a specialized
111 function in the removal of terminal introns to prevent nuclear export of pre-mRNAs
112 and this could be a mechanism to fine-tune gene expression under stress conditions.

113 # Results

114 **LUC7 proteins, a family of conserved nuclear zinc-finger / arginine-serine (RS)**
115 **proteins, redundantly control plant development**

116 *LUC7* stands for *Lethal Unless CBC 7* and was first identified in a screen for
117 synthetic lethality in a yeast strain lacking the cap-binding complex (CBC), which is
118 involved in RNA processing (Fortes *et al.*, 1999b; Gonatopoulos-Pournatzis &
119 Cowling, 2014; Sullivan & Howard, 2016). All LUC7 carry a C_3H and a C_2H_2-type
120 zinc-finger, which are located in the conserved LUC7 domain. LUC7 proteins from
121 higher eukaryotes usually contain an additional C-terminal Arginine/Serine-rich (RS)
122 domain, which is known to be involved in mediating protein-protein interactions (Heim
123 *et al.*, 2014; Puig *et al.*, 2007; Webby *et al.*, 2009). *Arabidopsis thaliana* encodes
124 three *LUC7* genes (*AthLUC7A*, *AthLUC7B* and *AthLUC7RL*), which are separated in
125 two clades: *LUC7A/B* and *LUC7RL* (Figure 1A and S1). AthLUC7RL is more similar
126 to its yeast homologs and lacks a conserved stretch of 80 amino acids of unknown
127 function present in AthLUC7A and AthLUC7B (Figure S1). A phylogenetic analysis
128 revealed that algae contain a single *LUC7* gene belonging to the LUC7RL clade
129 reinforcing the idea that LUC7RL proteins are closer to the ancestral LUC7 than
130 LUC7A/B. In the moss *Physcomitrella* and in the fern *Selaginella* one can find
131 proteins belonging to both clades, suggesting that the split into *LUC7RL* and
132 *LUC7A/B* occurred early during the evolution of land plants.

133 In order to understand the function of the Arabidopsis U1 snRNP, we analyzed
134 T-DNA insertion lines affecting *LUC7* genes (Figure 1B). Single and double *luc7*
135 mutants were indistinguishable from wild-type plants (WT) (Figure S2). However,
136 *luc7* triple mutant exhibit a wide range of developmental defects, including dwarfism
137 and reduced apical dominance (Figure 1C-E). To test whether the impairment of
138 *LUC7* functions were indeed responsible for the observed phenotypes, we

139 reintroduced a wild-type copy of *LUC7A*, *LUC7B* and *LUC7RL*, respectively, in the
140 *luc7* triple mutant. Each of the *LUC7* genes was sufficient to restore the phenotype of
141 the *luc7* triple mutant (Figure 1E). These results reveal that the phenotype observed
142 in this mutant is attributable to the impairment of *LUC7* function and it suggests that
143 *LUC7* genes act redundantly to control *Arabidopsis* growth and development.
144

145 **LUC7 is a U1 snRNP component in plants**

146 The composition of the U1 snRNP subcomplex is known in yeast and metazoans but
147 not in plants (Koncz *et al.*, 2012; Will & Luhrmann, 2001). Therefore, we asked
148 whether LUC7 is also an U1 component in Arabidopsis. Due to the fact that our
149 genetic analyses of *luc7* mutants suggest that LUC7 proteins act largely redundant,
150 we focused our further analyses mainly on a single LUC7 protein, LUC7A.

151 A protein that is part of the U1 complex is tightly associated with U1 specific
152 components such as the U1 snRNA. To test whether LUC7 is found in a complex
153 with the U1 snRNA, we performed RNA immunoprecipitation (RIP) experiments using
154 a *luc7 triple* mutant carrying a functional *pLUC7A:LUC7A-YFP* rescue construct
155 (Figure S3). LUC7A-YFP co-immunoprecipitated U1 snRNA, but not two unrelated,
156 but abundant RNAs, U3 snoRNA and *ACTIN* mRNA (Figure 2A). Also small amounts
157 of U2 snRNA associated with LUC7A-YFP, which is in agreement with the fact that
158 U1 and U2 snRNP directly interact to form spliceosomal complex A (Figure 2A).
159 These results strongly suggest that Arabidopsis LUC7 is a bona fide U1 snRNP
160 component.

161 Next we analyzed the subcellular localization of LUC7A and its co-localization
162 with a core U1 snRNP subunit. LUC7A localized to the nucleus, but not to the
163 nucleolus in *Arabidopsis* plants containing the pLUC7A:LUC7A-YFP rescue construct
164 (Figure 2B). In addition, LUC7A partially co-localized with U1-70K in the nucleoplasm

165 when transiently expressed in *Nicotiana benthamiana* (Figure 2C). Similar results
166 were obtained for LUC7RL, the Arabidopsis LUC7 most distant in sequence to
167 LUC7A (Figure 2C). Unlike U1-70K, LUC7A and LUC7RL did not form distinct
168 speckles in the nucleus and were evenly localized in the nucleoplasm (Figure 2C).

169 To further test whether LUC7A associates *in planta* with known U1 snRNP
170 core components, we purified LUC7A-containing complexes. For this, we used
171 pLUC7A:LUC7A-YFP complemented lines and as controls wild-type plants and
172 transgenic lines expressing free GFP. The mass spectrometry (MS) analysis
173 revealed that LUC7 is indeed found in a complex with core U1 snRNP proteins U1-A
174 and U1-70K (Figure 2D, Table S1). Furthermore, we detected peptides
175 corresponding to the spliceosomal complex E components U2AF35 and U2AF65,
176 further suggesting that LUC7 proteins are involved in very early steps of the splicing
177 cycle (Figure 2D) Additional proteins known to be involved in splicing and general
178 RNA metabolism including several serine-arginine (SR) proteins (SR30, SCL30A,
179 SCL33), SR45 and SERRATE (SE) were found in LUC7A-containing complexes
180 (Figure 2D). Interestingly, LUC7A was also associated with regulatory proteins,
181 among them several kinases (Figure 2D, Table S1). Taken together, our data show
182 that Arabidopsis LUC7 is an U1 snRNP protein and imply that LUC7 function is
183 regulated by kinases.

184

185 ***LUC7* effects on the Arabidopsis coding and non-coding transcriptome**

186 In order to identify misregulated and misspliced genes in luc7 mutants, we performed
187 an RNA-sequencing (RNA-seq) analysis with three biological replicates. We decided
188 to use 7 days old WT and luc7 triple mutant seedlings. At this age, luc7 triple mutant
189 and WT seedlings are morphologically similar and therefore, changes in transcript
190 levels and splicing patterns most likely reflect changes caused by LUC7s

191 impairments and are not due to different contribution of tissues caused by, for
192 instance, a delay in development or/and different morphology (Figure S4).
193 An analysis of differentially expressed genes revealed that 840 genes are up-
194 and 703 are downregulated in *luc7* mutants when compared to WT. The majority of
195 genes that change expression were protein-coding genes (Figure 3A). Nevertheless,
196 non-coding RNAs genes (ncRNAs) were significantly enriched among the *LUC7*
197 affected genes ($p < 0.05$, hypergeometric test), although the overall number of
198 ncRNA affected in *luc7* triple mutants is relatively small (Figure 3A, B). Previous
199 studies implied that the U1 snRNP regulates microRNA (miRNA) biogenesis
200 (Bielewicz *et al.*, 2013; Knop *et al.*, 2016; Schwab *et al.*, 2013; Stepien *et al.*, 2017).
201 However, the expression of *MIRNA* genes was not affected in *luc7* triple mutants
202 (Figure 3A). In addition, quantification of mature miRNA levels revealed that all tested
203 miRNAs did not change abundance in *luc7* triple mutant (Figure 3C). These results
204 show that *LUC7* genes affect the expression of protein-coding genes and a subset of
205 ncRNAs, but are not involved in the miRNA pathway.
206

207 **Arabidopsis *LUC7* function is important for constitutive and alternative**
208 **splicing**

209 Because LUC7 proteins are U1 snRNP components, we ask whether misspliced
210 transcripts accumulate in the *luc7* triple mutant. In total, we identified 645 differential
211 splicing events in *luc7* triple mutant compared to WT. We detected a large number of
212 intron retention events (Figure 4A). RT-PCR experiments with oligonucleotides
213 flanking selected intron retentions events confirmed the RNA-seq data (Figure 4B).
214 These results suggest that lack of the U1 snRNP component LUC7 impairs intron
215 recognition. Interestingly, we also identified a large number of exons that are
216 included in the *luc7* triple mutant when compared to WT, as well as cases of

217 alternative 5' and 3' splice site selection (Figure 4A-F). Some of these affected
218 splicing events generate transcript variants that did not exist in WT (e.g. *At2g32700*
219 Figure 4C). On the contrary, in other cases the *luc7* triple mutant lacked specific
220 mRNA isoforms, which exist in wild-type plants (e.g. *At1g10980*, *At4g32060*), or the
221 ratio of two different isoforms was altered in *luc7* triple mutant when compared to WT
222 (e.g. *At3g17310*, *At5g16715*, *At5g48150*, *At2g11000*) (Figure 4D-F). These results
223 show that Arabidopsis U1 snRNP proteins LUC7 are involved in constitutive and
224 alternative splicing.

225 Next, we checked whether splicing changes observed in *luc7* triple mutant are
226 actually due to the loss of only a specific *LUC7* gene or whether *LUC7* genes act
227 redundantly. To test this, we analyzed the splicing pattern of several mRNAs in *luc7*
228 single, double and triple mutants. Some splicing defects were detectable even in *luc7*
229 single mutants (Figure S5), but the degree of missplicing increased in *luc7* double
230 and triple mutants suggesting that LUC7 proteins act additively on these introns (e.g.
231 *At5g16715*). Some splicing defects occurred only in *luc7* triple mutants, implying that
232 LUC7 proteins act redundantly to ensure splicing of these introns (e.g. *At1g60995*).
233 Other splicing defects might more likely be due to the lack of LUC7A/B or LUC7RL.
234 For instance, intron removal of *At2g42010* more strongly relied on *LUC7RL*, while
235 removal of an intron in *At5g41220* preferentially depends on LUC7A/LUC7B (Figure
236 S5). These findings suggest that Arabidopsis *LUC7* genes function redundantly,
237 additively or specifically to ensure proper splicing.

238

239 **LUC7 proteins are preferentially involved in the removal of terminal introns**

240 In yeast, LUC7 connect the CBC with the U1 snRNP and this interaction is important
241 for correct 5' splicing site selection (Fortes *et al.*, 1999a). In plants, the CBC
242 associates with SE, which plays a role in the splicing of cap-proximal first introns in

243 Arabidopsis (Laubinger *et al.*, 2008; Raczynska *et al.*, 2010; Raczynska *et al.*, 2013).
244 Thus, to test the relationship between LUC7 and the CBC/SE, we analyzed the
245 splicing patterns of LUC7 dependent introns in *cbc* mutants (*cbp20* and *cbp80*) and
246 *se-1* by RT-PCR. All tested introns retained in *luc7* triple mutant were correctly
247 spliced in *cbc* and *se* mutants (Figure 5A). Conversely, first introns that are partially
248 retained in *cbp20, cbp80* and *se-1* mutants were completely removed in the *luc7*
249 triple mutant (Figure 5B). These observations suggest that the functions of LUC7 and
250 CBC/SE in splicing of the selected introns do not overlap.

251 Next, we asked whether LUC7 has a preference for promoting splicing of cap-
252 proximal first introns as it has the CBC/SE complex. We classified retained introns in
253 *luc7* triple mutants according to their position within the gene (first, middle or last
254 introns). Only genes with at least 3 introns were considered for this analysis. We
255 found a significant increase in retained last introns, but not first introns, in *luc7* triple
256 mutants (Figure 5C). Retention of terminal introns in *luc7* triple mutants was
257 confirmed by RT-PCR analysis (Figure 5D). Although the total number of retained
258 introns is higher in middle introns, the relative amount of retained middle introns in
259 *luc7* triple mutant was significantly reduced (Figure 5C). In summary, our data
260 revealed that (i) CBC/SE acts independently of LUC7 in splicing of cap-proximal
261 introns and that (ii) LUC7 proteins play an important role for the removal of certain
262 terminal introns.

263

264 **Splicing of LUC7-dependent terminal introns occurs independently of**
265 **polyadenylation**

266 The removal of terminal introns in yeast and metazoans can be tightly linked to
267 mRNA 3'end formation (Bentley, 2014; Cooke & Alwine, 2002; Cooke *et al.*, 1999;
268 Nesic & Maquat, 1994; Wong *et al.*, 2016). In some cases, polyadenylation precedes

269 splicing of terminal introns and the polyadenylation machinery plays an important role
270 in promoting splicing efficiency of terminal introns (Rigo & Martinson, 2008, 2009). To
271 investigate a putative link in between splicing of LUC7-dependent terminal introns
272 and polyadenylation, we isolated poly(A)+ and poly(A)- RNAs from WT and *luc7* triple
273 mutant and analyzed the splicing patterns of several LUC7-dependent terminal
274 introns (Figure 6A).

275 In WT, we found that unspliced isoforms of *At5g49840* and *At1g01860*
276 accumulated in poly(A)+ RNA fractions indicating that some polyadenylated mRNAs
277 still contained the LUC7 dependent terminal intron (Figure 6A). On the other hand,
278 the terminal introns of *At2g41560*, *At1g70480* and *At5g41220* were efficiently
279 removed in polyadenylated transcripts and high amounts of spliced mRNAs
280 accumulated in poly(A)- fractions. These observations suggest that these terminal
281 introns were efficiently removed before addition of the polyA-tail (Figure 6A). From
282 these results we conclude that LUC7-dependent introns can be removed before or
283 after polyadenylation. When we compared the splicing patterns in WT and *luc7* triple
284 mutant, we found that the splicing efficiency of some introns in *luc7* mutants was
285 already reduced in poly(A)- fractions (e.g. *At1g01860*). The splicing efficiency of
286 other terminal introns was affected only in poly(A)+ fractions (e.g. *At1g70480*). These
287 results further suggest that certain mRNAs require LUC7 function for efficient intron
288 removal before, other mRNAs after the addition of the poly(A)-tail.

289

290 **mRNAs harboring unspliced LUC7-dependent terminal introns remain in the**
291 **nucleus and escape NMD**

292 When introns are retained, the resulting mRNA can contain a premature stop codon
293 and a long 3'UTR, which are hallmarks of NMD targets (Drechsel *et al.*, 2013; Kalyna
294 *et al.*, 2012; Shaul, 2015). To check whether mRNAs containing a retained LUC7-

295 dependent terminal intron are NMD substrates, we analyzed their splicing patterns in
296 two mutants impaired in NMD, *lba-1* and *upf3-1*. If unspliced isoforms were indeed
297 NMD targets, we would expect their abundance to be increased in NMD mutants.
298 Interestingly, we did not observe any change between WT and *upf* mutants (Figure
299 6B). Thus, we conclude that retained LUC7-dependent terminal introns do not trigger
300 degradation via the NMD pathway.

301 NMD occurs in the cytoplasm and RNAs can escape NMD by not being
302 transported from the nucleus to the cytosol (Gohring *et al.*, 2014). We therefore
303 checked in which cellular compartment mRNAs with spliced and unspliced LUC7-
304 dependent terminal introns accumulate. To do this, we isolated total, nuclear and
305 cytosolic fractions from wild-type and *luc7* triple mutant plants and performed RT-
306 PCR analyses (Figure 6C). Spliced mRNA isoforms accumulated in the cytosol,
307 whereas mRNAs containing the unspliced terminal introns were found in nuclear
308 fractions (Figure 6C). These results indicate that retention of terminal introns
309 correlates with trapping mRNAs in the nucleus and suggest that splicing of LUC7-
310 dependent terminal introns is essential for mRNA transport to the cytosol.

311

312 **Splicing of LUC7-dependent terminal introns can be modulated by stress**

313 Our results revealed that a subset of terminal introns requires LUC7 proteins for
314 efficient splicing, and that splicing of these introns is a prerequisite for nuclear export.
315 This mechanism could serve as a nuclear quality control step to prevent that
316 unspliced mRNAs are exported prematurely. Interestingly, a GO analysis of genes
317 containing LUC7 dependent terminal introns indicated an enrichment for stress
318 related genes (Figure S6). This prompted us to speculate that nuclear retention of
319 mRNAs could be exploited as a regulatory mechanism to fine-tune gene expression
320 under stress conditions. To test this hypothesis, we decided to check the splicing of

321 LUC7-dependent terminal introns in WT under stress condition. We chose cold stress
322 because it was suggested that U1 snRNP functionality is impaired under cold
323 condition (Schlaen *et al.*, 2015). To quantify the amount of unspliced isoform in cold
324 condition, we designed qPCR-primers specific to unspliced isoform and total RNA
325 and calculate the ratio unspliced/total of LUC7-dependent terminal introns in four
326 genes (*At1g70480*, *At2g41560*, *At5g44290* and *At5g41220*). Three of these genes
327 significantly accumulated unspliced transcripts in responses to cold treatment
328 demonstrating that cold stress modulates the splicing efficiency of LUC7-dependent
329 terminal introns (Figure 7A).
330

331 **Cold and salt stress preferentially affects splicing of first and terminal introns**

332 To investigate whether terminal intron retention is a general feature of plant stress
333 transcriptomes, we performed a global analysis of intron retention under stress
334 condition. We made use of publically available RNA-seq data sets from Arabidopsis
335 plants treated with cold and salt stress (Ding *et al.*, 2014; Schlaen *et al.*, 2015). We
336 identified stress-regulated intron retention events, filtered for genes containing three
337 or more introns, and assigned retained introns based on their position within the
338 transcript (first, middle or terminal intron). The relative amount of first, middle and
339 terminal introns among retained introns under stress conditions was compared to the
340 relative amount of introns among all expressed genes. We found that up- and down-
341 regulated intron retention events during cold and salt stress were significantly
342 enriched in first and terminal introns (Figure 7B-C, Figure S7). These results show
343 that first and terminal introns are preferentially subjected to alternative splicing
344 regulation under stress conditions. We observed a higher proportion of retained first
345 and last introns in two different stresses condition and varying stress intensities and
346 durations (Figure 7B-C, Figure S7). Thus, our data strongly suggest that regulated

347 splicing of first and terminal introns widely contributes to shaping plant
348 transcriptomes under stress conditions.

349 # Discussion

350 **Functions of the Arabidopsis U1 snRNP component LUC7**

351 For this study, we generated an Arabidopsis mutant deficient in the U1 snRNP
352 component LUC7 and dissected the genome-wide effects of LUC7 impairment on the
353 Arabidopsis transcriptome. Our results show that LUC7 proteins are *bona-fide* U1
354 components acting mainly redundantly. The reduction of U1 function in the *luc7* triple
355 mutant affects constitutive splicing. A large number of introns are retained in *luc7*
356 triple mutant, suggesting that without a proper recognition of the 5'ss, splicing of the
357 affected introns is impaired. Our results also show that exon-skipping events are
358 impaired in *luc7* triple mutant, revealing that a functional plant U1 snRNP is essential
359 for exon definition. In addition, we show that *luc7* triple mutant affect alternative
360 splicing also by influencing events of alternative 5' and 3' splice site. This implies that
361 the U1 snRNP does not only affect 5' splice site usage, it might also indirectly
362 regulate usage of 3' splice sites via its interaction with U2AFs and the U2 snRNP
363 (Hoffman & Grabowski, 1992; Shao *et al.*, 2012). The functions of LUC7 proteins on
364 the Arabidopsis transcriptome are likely to be underestimated, because misspliced
365 mRNAs in *luc7* mutants might contain hallmarks of NMD and are therefore rapidly
366 turned over and escape detection. Analysis of *luc7* mutants combined with mutations
367 in NMD factors would help to uncover the full set of splicing events affected by LUC7.
368 One has also to consider that U1 snRNP independent splicing has been described in
369 animals, indicating that not all introns require the U1 complex for efficient intron
370 removal (Fukumura *et al.*, 2009). The degree of U1-independent splicing in plants
371 remains to be elucidated.

372 Duplications among genes encoding for U1 snRNP proteins, such as the
373 LUC7 genes, might suggest that U1 accessory genes have undergone sub- and
374 neofunctionalization. Furthermore, the Arabidopsis genome encodes 14 potential U1

375 snRNAs, which slightly differ in sequence (Wang & Brendel, 2004). Therefore, the
376 plant U1 snRNP presumably does not exist as a single complex, but exists as
377 different sub-complexes exhibiting distinct specificities and functions. In metazoans,
378 the existence of at least four different U1 snRNP subcomplex has been suggested
379 (Guiro & O'Reilly, 2015; Hernandez *et al.*, 2009). Specific combinations of plant U1
380 protein family members and U1 snRNAs could generate an even higher number of
381 such U1 subcomplexes, which could be responsible for specific splicing events. Our
382 results show that LUC7 can act redundantly, but can also fulfill specific functions,
383 suggesting that LUC7 complexes specifically act on certain pre-mRNAs. In this
384 regard, it is important to note that an additional short stretch of aminoacids separates
385 the two zinc-finger RNA binding domains in LUCA and LUC7B. Changing the space
386 in between RNA binding domains affects substrate specificities and could explain
387 different functions among LUC7 proteins (Chen & Varani, 2013).

388 Interestingly, *luc7* triple mutant showed a significant higher retention rate of
389 terminal introns compared to first or middle introns. This was surprising because
390 LUC7 was initially found to act in concert with the CBC, a complex involved in the
391 removal of cap-proximal first introns, but not of last introns (Lewis *et al.*, 1996). Often,
392 the removal of terminal introns is coupled to polyadenylation (Cooke & Alwine, 2002;
393 Cooke *et al.*, 1999; Rigo & Martinson, 2008). However, our analysis suggests that
394 splicing of LUC7-dependent terminal introns occurs in some cases independently of
395 polyadenylation because some introns were removed after the addition of the poly(A)
396 tail. Interestingly, we detected the pre-mRNA cleavage/polyadenylation factor
397 AT4G25550 as part of LUC7A complexes, suggesting that an interaction between
398 LUC7 and 3' end formation complexes may contribute to the specific functions of
399 LUC7 in terminal intron splicing.
400

401 **Potential functions of terminal intron retention in plants**

402 Targeting a transcript to NMD can be triggered by two mechanisms: For the first one,
403 it requires the deposition of an exon-junction-complex (EJC) downstream of the
404 retained intron which causes a premature stop codon. For the second one, mRNAs
405 containing a long 3'UTR (≥300 - 350 nt) are degraded via the NMD pathway
406 (Drechsel *et al.*, 2013; Kalyna *et al.*, 2012; Kervestin & Jacobson, 2012; Shaul,
407 2015). Retained terminal introns are then special because their detection solely relies
408 on the length of the 3'UTR. Transport of mRNAs containing unspliced terminal
409 introns, especially those which feature a relatively short 3'UTR, can be detrimental
410 and has to be tightly controlled. Interestingly, we found that splicing of LUC7-
411 dependent terminal introns is required for transport of mRNAs from the cytosol to the
412 nucleus. The fact that we cannot detect unspliced transcript in the cytosol suggests a
413 nuclear retention mechanism for such mRNAs. One possibility is that LUC7
414 dependent terminal introns might contain binding sites for specific trans-regulatory
415 factors that upon binding inhibit export. Polypyrimidine tract-binding protein 1 (PTB1)
416 is a prime candidate for such a trans-regulatory protein, because binding of PTB1 to
417 introns represses nuclear export of certain RNAs (Roy *et al.*, 2013; Yap *et al.*, 2012).

418 Nuclear retention of unspliced mRNAs is not limited to terminal introns and
419 might be a much more general mechanism to escape NMD and to regulate gene
420 expression (Wong *et al.*, 2016). In plants, some specific transcript isoforms have
421 been detected only in the nucleus, but not in the cytosol (Gohring *et al.*, 2014). Also
422 in metazoans, intron retention might have a more general role in regulating gene
423 expression (Naro *et al.*, 2017; Pimentel *et al.*, 2016; Yap *et al.*, 2012). The so-called
424 detained introns are evolutionary conserved, NMD insensitive and retained in the
425 nucleus (Boutz *et al.*, 2015). The functional importance of intron retention was also

426 suggested in the fern *Marsilea vestita*, in which many mRNAs contain introns that are
427 only spliced shortly before gametophyte development (Boothby *et al.*, 2013).
428 We found that LUC7-dependent splicing of terminal introns can be modulated
429 by cold stress. Because retention of these introns causes nuclear trapping, it is
430 prompting to speculate that environmental cues affect splicing and nuclear retention
431 of mRNAs. Such a mechanism would regulate the amount of translatable mRNAs in
432 the cytosol in a cost-efficient and rapid manner. Because the RS domains of LUC7
433 proteins are phosphorylated and we identified several kinases as LUC7A interactors,
434 stress-induced changes in phosphorylation might play a role in regulating LUC7
435 proteins and U1 snRNP function (Durek *et al.*, 2010; Heazlewood *et al.*, 2008). This
436 idea is supported by the observation that stress signaling triggered by the
437 phytohormone ABA results in phosphorylation of several splicing factors (Umezawa
438 *et al.*, 2013; Wang *et al.*, 2013)
439 In general, our analysis suggests that first and terminal introns are hotspots
440 for regulated splicing under stress conditions. First and last introns are close to the 5'
441 cap and the polyA tail, respectively. These positions might offer more possibilities for
442 splicing regulation via crosstalk between the splicing machinery and factors involved
443 in capping and cleavage/polyadenylation. We are just at the beginning of
444 understanding the importance of intron retention in gene regulation. Future
445 identification of cis- and trans-regulatory factors involved in the regulation of terminal
446 intron splicing will shed additional light on this layer of gene expression.
447

448 **Material and Methods**

449

450 **Plant material and growth conditions**

451 All mutants were in the Columbia-0 (Col-0) background. *luc7a-1* (SAIL_596_H02)
452 and *luc7a-2* (SAIL_776_F02), *luc7b-1* (SALK_144681), *luc7rl-1* (SALK_077718) and
453 *luc7rl-2* (SALK_130892C) were isolated by PCR-based genotyping (Table S2). *luc7*
454 double and triple mutants were generate by crossing individual mutants. All other
455 mutants used in this study (*abh1-285*, *cbp20-1*, *se*-1, *lba-1* and *upf3-1*) were
456 described elsewhere (Hori & Watanabe, 2005; Laubinger *et al.*, 2008; Papp *et al.*,
457 2004; Prigge & Wagner, 2001; Yoine *et al.*, 2006). The line expressing GFP was
458 generated using the vector pBinarGFP and was kindly provided by Dr. Andreas
459 Wachter (Wachter *et al.*, 2007). For complementation analyses, *pLUC7A:LUC7A-*
460 *FLAG*, *pLUC7B:LUC7B-FLAG*, *pLUC7RL:LUC7RL-FLAG* and *pLUC7A:LUC7A-YFP*
461 constructs were introduced in *luc7* triple mutant by Agrobacterium-mediated
462 transformation (Clough & Bent, 1998). All plants were grown on soil in long days
463 conditions (16-h light/8-h dark) at 20°C/18°C day/night. The size of *luc7* mutants was
464 assessed by measuring the longest rosette leaf after 21 days. For all molecular
465 studies, seeds were surface-sterilized, plated on 1/2 MS medium with 0.8%
466 phytoagar and grown for 7 days in continuous light at 22°C. For the cold treatment,
467 plates with *Arabidopsis* seedlings were transferred to ice-water for 60 min.

468

469 **Plasmid constructions and transient expression analyses**

470 For the expression of C-terminal FLAG- and YFP-tagged LUC7 proteins expressed
471 from their endogenous regulatory elements, 2100 bp, 4120 bp and 2106 bp upstream
472 of the ATG start codon of *LUC7A*, *LUC7B* and *LUC7RL*, respectively, to the last
473 coding nucleotide were PCR-amplified and subcloned in pCR8/GW/TOPO®

474 (Invitrogen). Oligonucleotides are listed in Table S2). Entry clones were recombined
475 with pGWB10 and pGWB540 using Gateway LR clonase II (Invitrogen) to generate
476 binary plasmids containing *pLUC7A:LUC7A-FLAG*, *pLUC7B:LUC7B-FLAG*,
477 *pLUC7RL:LUC7RL-FLAG* and *pLUC7A:LUC7A-YFP*. For the co-localization studies,
478 entry vector containing the coding sequence of U1-70k was recombined with
479 pGWB654 for the expression of *p35S:U1-70k-mRFP* (Nakagawa *et al.*, 2007).
480 Agrobacterium-mediated transient transformation of *Nicotiana benthamiana* plants
481 was conducted as following. Overnight Agrobacterium culture were diluted in 1:6 and
482 grown for 4 hours at 28°C. After centrifugation, pellets were ressuspended in
483 infiltration medium (10mM $MgCl_2$, 10mM MES-KOH pH 5.6, 100 µM Acetosyringone).
484 The OD 600nm was adjusted to 0.6-0.8 and samples were mixed when required. *N.*
485 *benthamiana* were infiltrated and subcellular localization was checked after 3 days.
486 Subcellular localization of fluorescent proteins was analyzed by confocal microscopy
487 using a Leica TCS SP8.
488

489 **Phylogenetic analysis**

490 AthLUC7A (AT3G03340) protein sequence was analyzed in Interpro
491 (https://www.ebi.ac.uk/interpro/) to retrieve the Interpro ID for the conserved Luc7-
492 related domain (IPR004882). The sequence for *Saccharomyces cerevisiae* (strain
493 ATCC 204508_S288c) was obtained in Interpro. Plants sequences were extracted
494 using BioMart selecting for the protein domain IPR004882 on Ensembl Plants
495 (http://plants.ensembl.org/). The following genomes were included in our analyses:
496 *Amborella trichopoda* (AMTR1.0 (2014-01-AGD)); *Arabidopsis thaliana* (TAIR10
497 (2010-09-TAIR10)); *Brachypodium distachyon* (v1.0); *Chlamydomonas reinhardtii*
498 (v3.1 (2007-11-ENA)); *Physcomitrella patens* (ASM242v1 (2011-03-Phypa1.6));
499 *Selaginella moellendorffii* (v1.0 (2011-05-ENA)); *Oryza sativa Japonica* (IRGSP-1.0);

500 and *Ostreococcus lucimarinus* genes (ASM9206v1). The phylogenetic analysis was
501 performed in Seaview (Version 4.6.1) using Muscle for sequence alignment.
502 Maximum likehood (PhYML) was employed with 1000 bootstraps (Gouy *et al.*, 2010).
503

504 **RNA extractions, RT-PCR and qRT-PCR**

505 RNAs extractions were performed with Direct-zol™ RNA MiniPrep Kit (Zymo
506 Research). Total RNAs were treated with DNAse I and cDNA synthesis carried out
507 with RevertAid First Strand cDNA Synthesis Kit (Thermo Scientific) using usually
508 oligo dT primers or a mixture of hexamer and miRNA-specific stem-loop primers
509 (Table S2). Standard PCRs for the splicing analysis were performed with DreamTaq
510 DNA Polymerase (Thermo Scientific). Quantitative RT-PCR (qRT-PCR) was
511 performed using the Maxima SYBR Green (Thermo Scientific) in a Bio-Rad CFX 384.
512 For all qPCR-primers, primer efficiencies were determined by a serial dilution of
513 cDNA template. The relative expressions were calculated using the 2ˆ(-ΔΔCT)
514 method with *PP2A* or *ACTIN* as controls. For the qRT-PCR to detect splicing ratio
515 changes under cold condition, the ratio 2ˆ(-ΔCTunspliced)/2ˆ(-ΔCTtotal RNA) was
516 calculated separately for each replicate and t-test was performed before calculating
517 the relative to WT. Primers used for PCR and qRT-PCR are listed Table S2. For
518 RNA-sequencing analysis, polyA RNAs were enriched from 4 µg of total RNAs using
519 NEBNext Oligo $d(T)_{25}$ Magnetic Beads (New England Biolabs). The libraries were
520 prepared using ScriptSeq™ Plant Leaf kit (Epicentre) following the manufacturer's
521 instruction. Single end sequencing was performed on an Illumina HiSeq2000.
522 Sequencing data were deposited at Gene Expression Omnibus under accession
523 number GSE98779.
524

525 **Isolation of poly(A)- and poly(A)+ fractions**

526 RNAs were extracted from seedlings and treated with DNAseI as described above.
527 After the DNAse treatment, samples were cleaned up using RNA Clean &
528 Concentrator-5 (Zymo Research).Two replicates were performed 1.5 - 3 µg of total
529 RNA was used for the fractionation. The poly(A) fractions were prepared using
530 NEBNext Oligo $d(T)_{25}$ Magnetic Beads (New England Biolabs). Each fraction was
531 purified twice. For the poly A(-) fractions, large sample volumes were concentrated
532 with RNA Clean & Concentrator-5. cDNA synthesis was carried out with random
533 hexamer primers as described above.
534

535 **Subcellular fractionation**

536 Two grams of seedlings were ground in N_2 liquid and resuspended in 4 ml of Honda
537 buffer (0.44 M sucrose, 1.25% Ficoll 400, 2.5% Dextran T40, 20 mM HEPES KOH
538 pH 7.4, 10 mM $MgCl_2$, 0.5% Triton X-100, 5 mM DTT, 1 mM PMSF, protease
539 inhibitor cocktail [ROCHE] supplemented with 40U/ml of Ribolock®). The
540 homogenate was filtered through 2 layer of Miracloth, which was washed with 1ml of
541 Honda Buffer. From the filtrate, 300 µl was removed as “total” fraction and kept on
542 ice. Filtrates were centrifuged at 1,500 *g* for 10 min, 4°C for pelleting nuclei and
543 supernatants were transferred to a new tube. Supernatants were centrifuged at 13
544 000 x g, 4 °C, 15 min and 300 µl were kept on ice as cytoplasmic fraction. Nuclei
545 pellets were washed five times in 1 ml of Honda buffer (supplemented with 8U/ml of
546 Ribolock®, centrifugation at 1,800 *g* for 5 min. The final pellet was resuspended in
547 300 µl of Honda buffer. To all the fractions (total, cytoplasmic and nuclei), 900 µl of
548 TRI Reagent (Sigma) was added. After homogenization, 180 µl of chloroform was
549 added and samples were incubated at room temperature for 10 min. After
550 centrifugation at 10 0000 rpm for 20 min, 4°C, the aqueous phase were transferred to
551 a new tube and RNA extracted with Direct-zol™ RNA MiniPrep Kit (Zymo Research).

552 The organic phase was collected and proteins were isolated according to
553 manufacturer's instructions (TRI Reagent). cDNA synthesis with random primes was
554 performed as above. Proteins extracted were analyzed by standard western blot
555 techniques using the following antibodies: H3 (~ 17KDa / ab 1791, Abcam) and 60S
556 ribosomal (~ 23,7-29KDa / L13, Agrisera).
557

558 **RNA immunoprecipitation**

559 RNA immunoprecipitation (RIP) using WT and a *pLUC7A:LUC7A-eYFP* rescue line
560 was performed as described elsewhere with minor modifications (Rowley *et al.*, 2013;
561 Xing *et al.*, 2015). Isolated nuclei were sonicated in nuclear lysis buffer in a Covaris
562 E220 (Duty Cycle: 20%; Peak intensity: 140; Cycles per Burst: 200; Cycle time: 3').
563 RNAs were extracted using RNeasy Plant Mini Kit (QIAGEN) following the
564 manufacturer's instructions. The RNA were treated with DNAseI (Thermo Scientific)
565 and samples were split in half for the (-)RT reaction. cDNA synthesis were perform
566 with SuperScript™ III Reverse Transcriptase (Invitrogen). qRT-PCRs were performed
567 with QuantiNova™ SYBRR Green PCR (QIAGEN).
568

569 **RNA-seq libraries: Mapping, differential expression analysis and splicing**
570 **analysis**

571 RNA-seq reads for each replicate were aligned against the *Arabidopsis thaliana*
572 reference sequence (TAIR10) using tophat (v2.0.10, -p2, -a 10, -g 10, -N 10, --read-
573 edit-dist 10, --library-type fr-secondstrand, --segment-length 31, -G TAIR10.gff). Next,
574 cufflinks (version 2.2.1) was used to extract FPKM counts for each expressed
575 transcript generating a new annotation file (transcripts.gtf), where the coordinates of
576 each expressed transcript can be found. Cuffcompare (version 2.2.1) was then used
577 to generate a non-redundant annotation file containing all reference transcripts in

578 addition to new transcripts expressed in at least one of the nine samples
579 (cuffcmp.combined.gtf). The differential expression analysis was performed with
580 cuffdiff (version 2.2.1) between wt/*luc7* triple using the annotation file generated by
581 cuffcompare (FDR<2 and FC>0,05). For the splicing analysis, the same alignment
582 files generated by tophat and annotation files generated by cuffcompare
583 (cuffcmp.combined.gtf) were used as input for MATS (version 3.0.8) in order to test
584 for differentially spliced transcripts (Shen *et al.*, 2014).
585

586 **Global analysis of intron regulation under stress conditions**

587 For the analyses of intron retention under stress conditions, published data sets were
588 analyzed (accession numbers SRP035234 and SRP049993) (Ding *et al.*, 2014;
589 Schlaen *et al.*, 2015). Reads were aligned to the *Arabidopsis thaliana* Ensembl3 33
590 genome and to the annotation GTF file (ftp://ftp.ensemblgenomes.org/pub/release-
591 33/plants/fasta/arabidopsis_thaliana/dna/Arabidopsis_thaliana.TAIR10.dna.toplevel.f
592 a.gz, ftp://ftp.ensemblgenomes.org/pub/release-33/plants/gtf/
593 arabidopsis_thaliana/Arabidopsis_thaliana.TAIR10.33.gtf.gz) using TopHat2 applying
594 following parameters: tophat2 -p 10 -i 10 -I 1000 -G
595 Arabidopsis_thaliana.TAIR10.33.gtf Arabidopsis_thaliana.TAIR10.dna.toplevel.fa.
596 After alignment, mock-treated samples were used to generate an expressed
597 background for the respective dataset using featureCounts from the Rsubread
598 package (Kersey *et al.*, 2016; Kim *et al.*, 2013; Liao *et al.*, 2013). Read numbers and
599 gene lengths per genes (featureCounts -T 6 -R -p -F GTF -J -G
600 Arabidopsis_thaliana.TAIR10.dna.toplevel.fa -a Arabidopsis_thaliana.TAIR10.33.gtf)
601 were collected and TPM values were calculated using an in-house script. Log_2
602 transformed values of expressed genes were visualized with ggplot2 version 2.1.0,

603 and based on the density plot, threshold of expressed genes was defined as
604 $TPM_{expressed} > 0.6$.
605 Intron retention events were identified using rMATS with the following
606 parameters: python RNASeq-MATS.py -b1 untreated.bam -b2 treated.bam -gtf
607 Arabidopsis_thaliana.TAIR10.33.gtf -o output_dir -t paired -len 101 (Shen *et al.*,
608 2014). After filtering the outputs (p value < 0.05, FDR < 0.05), we categorize introns
609 based on their position and annotation. In case of a few ambiguous hits, they were
610 manually recategorized. For the categorization of introns in first, middle and last
611 introns, we used the GTF annotation file (Ensembl 33) and selected genes with 3 or
612 more introns and TPM > 0.6. The intron distribution of all expressed genes served as
613 a background reference, to which the distribution of retained introns under stress
614 conditions was compared. To test for significance of changes in intron distribution,
615 Fisher's exact test was employed since we assumed a normal distribution.
616
617 **GO Analysis**
618 GO analysis was performed in Bar Utoronto (http://bar.utoronto.ca/ntools/cgi-
619 bin/ntools_classification_superviewer.cgi).
620
621 **Protein complex purification and mass spectrometry (MS) Analysis**
622 LUC7A immunoprecipitation was performed using a complemented line
623 *pLUC7A:LUC7A-eYFP* (line 20.3.1) and a transgenic *p35S:GFP* and WT as controls.
624 Four independent biological replicates were performed. Seedlings (4 g) were ground
625 in N_2 liquid and respuspended in 1 volumes of extraction buffer (50 mM Tris-Cl pH
626 7.5, 100 mM NaCl, 0,5% Triton X-100, 5% Glycerol, 1mM PMSF, 100 µM MG132,
627 Complete Protease Inhibitor Cocktail EDTA-free [Roche] and Plant specific protease
628 Inhibitor, Sigma P9599). After thawing, samples were incubated on ice for 30 min,

629 centrifuged at 3220 rcf for 30 min at 4°C and filtrated with two layers of Miracloth. For
630 each immunoprecipitation, 20 µl of GFP-trap (Chromotek) was washed twice with 1
631 ml of washing buffer (50 mM Tris-Cl pH 7.5, 100 mM NaCl, 0.2% Triton X-100) and
632 once with 0.5 ml of IP buffer. For each replicate, the same amount of plant extracts
633 (~5ml) were incubated with GFP-trap and incubated on a rotating wheel at 4°C for 3
634 hours. Samples were centrifuged at 800-2000 rcf for 1-2 min and the supernatant
635 discarded. GFP-beads were resuspended in 1 ml of washing buffer, transferred into a
636 new tube and washed 4 to 5 times. Then, beads were ressuspended in ~40 µl of 2x
637 Laemmili Buffer and incubated at 80°C for 10 min. Short gel purifications (SDS-
638 PAGE) were performed and gels slices were digested with Trypsin. LC-MS/MS
639 analyses were performed in two mass spectrometer. Samples from R10 to R14 were
640 analyzed on a Proxeon Easy-nLC coupled to Orbitrap Elite (method: 90min, Top10,
641 HCD). Samples from R15 to R17 were analysed on a Proxeon Easy-nLC coupled to
642 OrbitrapXL (method: 90min, Top10, CID). Samples from R18 to R20 analysis on a
643 Proxeon Easy-nLC coupled to OrbitrapXL (method: 130min, Top10, CID). All the
644 replicates were processed together on MaxQuant software (Version 1.5.2.8. with
645 integrated Andromeda Peptide search engine) with a setting of 1% FDR and the
646 spectra were searched against an *Arabidopsis thaliana* Uniprot database
647 (UP000006548_3702_complete_20151023.fasta). All peptides identified are listed in
648 Supplementary Table S1 and raw data were deposited publically (accession
649 PXD006127).

650

651 **Acknowledgments**

652 This work was supported by the Deutsche Forschungsgemeinschaft DFG (to S.L.,
653 LA2633-4/1), Coordenação de Aperfeiçoamento de Pessoal de Nível Superior

654 (CAPES - Brazil) for doctoral fellowship (to M.d.F.A.), the Max Planck Society (to
655 K.S.), the Max Planck Society Chemical Genomics Centre (CGC) through its
656 supporting companies AstraZeneca, Bayer CropScience, Bayer Healthcare,
657 Boehringer-Ingelheim and Merck (to S.L). We are grateful to Andreas Wachter
658 (ZMBP, University of Tuebingen, Germany) and members of the lab for critical
659 reading of the manuscript, Christa Lanz for her invaluable help with Illumina
660 sequencing, and Johanna Schröter and her team for excellent care of our plants,
661 Anja Hoffmann for excellent technical assistance, and Andreas Wachter (ZMBP,
662 University of Tuebingen, Germany), Tsuyoshi Nakagawa (Department of Molecular
663 and Functional Genomics, Center for Integrated Research in Science, Shimane
664 University, Matsue, Japan) and the Notthingham Arabidopsis Stock Centre for
665 providing seeds and DNA constructs.

666

667 ## Competing interests

668 The authors declare no competing interests.

669

670 ## Figure legends

671 **Figure 1: *Arabidopsis* LUC7 proteins redundantly control plant development**

672 **A:** Phylogenetic analysis of LUC7 proteins in the plant kingdom using
673 *Saccharomyces cerevisiae* as an external group.

674 **B:** Exon/intron structure of *Arabidopsis thaliana LUC7A*, *LUC7B* and *LUC7RL*.
675 Dotted lines indicate the positions of T-DNA insertions.

676 **C:** WT and *luc7* triple mutant plants 21 days (left) and 45 days (right) after
677 germination.

678 **D:** Length of the longest rosette leaf of 21 days-old WT, *luc7* single, double and triple
679 mutant plants growing under long day conditions. Leaves of 10-15 individual plants
680 were measured. Dots indicate individual data points. Error bars denote the SEM.
681 **E:** Complementation of *luc7a,b,rl* mutants by *LUC7A*, *LUC7B* and *LUC7RL* genomic
682 rescue constructs. Transformation of an "empty" binary vector served as a control.
683 Two independent transgenic lines for each construct are shown.
684
685 **Figure 2: *Arabidopsis* LUC7 is an U1 snRNP component**
686 **A:** RNA immunoprecipitation using a *pLUC7A:LUC7A-YFP, luc7a,b,rl* complemented
687 line. Proteins were immunoprecipitated using GFP-specific affinity matrix and RNAs
688 were extracted from the input and the immunoprecipitated. U1, U2, U3 snRNAs and
689 *ACTIN* RNA were quantified using qRT-PCR. Enrichment of the respective RNA in
690 *LUC7A:LUC7A-YFP luc7a,b,rl* transgenic lines was calculated over WT (negative
691 control). Error bars denote the range of two biological replicates.
692 **B:** Subcellular localization of LUC7A in *pLUC7A:LUC7A-YFP luc7a,b,rl* in
693 Arabidopsis transgenic plants. Roots of 9 day-old seedlings were analyzed using
694 confocal microscopy. Scale bar indicates 25 µm.
695 **C:** U1-70K-mRFP and LUC7A-YFP or LUC7RL-YFP proteins were transiently
696 expressed in *N. benthamiana*. The subcellular localization of mRFP and YFP fusion
697 proteins was analyzed using confocal microscopy. Scale bars indicate 10 µm and 25
698 µm for upper and lower panel, respectively.
699 **D:** List of some LUC7-associated proteins identified by MS.
700
701 **Figure 3: Mutations in *LUC7* results in misexpression of protein-coding and**
702 **non-coding genes, but not in *MIRNA* genes**
703 **A:** Differentially expressed genes in *luc7a,b,rl* mutant compared to WT.

704 **B,C:** qRT-PCR analysis of selected ncRNA **(B)** and miRNAs **(C)** in WT and
705 *luc7a,b,rl*. Error bars denote the SEM (n=3).
706
707 **Figure 4: Global analysis of splicing defects in *luc7* triple mutant.**
708 **A:** Classification of splicing events changes in *luc7* triple mutant compared to WT.
709 **B-F:** Coverage plots and RT-PCR validation experiments for selected splicing events
710 in WT and *luc7* triple mutant. Genomic DNA (gDNA) or water (-) served as a control.
711 Primers positions are indicated with gray arrows. IR, intron retention; ES, exon
712 skipping; Alt.3'SS, alternative 3'splicing site; Alt.5'SS, alternative 5'splicing site.
713
714 **Figure 5: LUC7 proteins have a pronounced effect on terminal intron splicing**
715 **A:** RT-PCR analysis of LUC7-dependent introns in WT, *luc7* triple mutant, *cbp80*,
716 *cbp20* and *se-1* mutants.
717 **B:** RT-PCR analysis of CBC/SE-dependent introns in WT, *luc7* triple mutant, *cbp80*,
718 *cbp20* and *se-1* mutants.
719 **C:** Classification of intron retention according to the intron position (first, middle, or
720 last). Only genes with 3 or more introns were considered for this analysis. Terminal
721 introns are significantly enriched among introns retained in *luc7* triple mutants
722 (Fischer test; two-side $p < 0.0016$).
723 **D:** RT-PCR analysis of genes carrying retained terminal introns in WT and *luc7* triple
724 mutants.
725
726 **Figure 6: mRNAs containing retained LUC7-dependent terminal introns are**
727 **NMD-insensitive and remain nuclear.**
728 **A:** Splicing patterns of mRNAs carrying LUC7-dependent terminal introns in poly(A)+
729 and poly(A)- fractions.

730 **B:** RT-PCR analysis of LUC7-dependent terminal introns in WT and NMD mutants
731 (*lba1* and *upf3-1*).
732 **C:** Splicing patterns of mRNAs isolated from total (T), cytosolic (C) and nuclear (N)
733 fractions.
734
735 **Figure 7: Splicing of LUC7 dependent terminal introns can be modulated by**
736 **stress.**
737 **A:** Seven days old WT seedlings were exposed to cold for 60 min. Splicing ratios
738 (unspliced/total RNA) of four genes featuring a LUC7-dependent terminal intron was
739 analyzed by qPCR. T-test was performed before calculating the relative to WT (*
740 p=0,0208, ** p =0,0095, *** p = 0.004).
741 **B-C:** Classification of intron retention events in cold- (B) and salt-treated plants (C)
742 The relative amount of retained/removed first, middle, and last intron in stress
743 samples was compared to the relative amount of first, middle, and last intron among
744 all expressed genes (normal distribution). Only genes with 3 or more introns were
745 considered for this analysis. * $p < 0.05$, ** $p < 0.01$, *** $p < 0.001$, **** $p < 0.0001$
746

747 # Literature

748 Almada, A. E., Wu, X., Kriz, A. J., Burge, C. B., & Sharp, P. A. (2013). Promoter
749 directionality is controlled by U1 snRNP and polyadenylation signals. *Nature,*
750 *499*(7458), 360-363. doi: 10.1038/nature12349
751 Bentley, D. L. (2014). Coupling mRNA processing with transcription in time and
752 space. *Nat Rev Genet, 15*(3), 163-175. doi: 10.1038/nrg3662
753 Berg, M. G., Singh, L. N., Younis, I., Liu, Q., Pinto, A. M., Kaida, D., Zhang, Z., Cho,
754 S., Sherrill-Mix, S., Wan, L., & Dreyfuss, G. (2012). U1 snRNP determines
755 mRNA length and regulates isoform expression. *Cell, 150*(1), 53-64. doi:
756 10.1016/j.cell.2012.05.029

757 Bielewicz, D., Kalak, M., Kalyna, M., Windels, D., Barta, A., Vazquez, F.,
758 Szweykowska-Kulinska, Z., & Jarmolowski, A. (2013). Introns of plant pri-
759 miRNAs enhance miRNA biogenesis. *EMBO Rep, 14*(7), 622-628. doi:
760 10.1038/embor.2013.62
761 Boothby, T. C., Zipper, R. S., van der Weele, C. M., & Wolniak, S. M. (2013).
762 Removal of retained introns regulates translation in the rapidly developing
763 gametophyte of Marsilea vestita. *Dev Cell, 24*(5), 517-529. doi:
764 10.1016/j.devcel.2013.01.015
765 Boutz, P. L., Bhutkar, A., & Sharp, P. A. (2015). Detained introns are a novel,
766 widespread class of post-transcriptionally spliced introns. *Genes Dev, 29*(1),
767 63-80. doi: 10.1101/gad.247361.114
768 Carvalho, R. F., Feijao, C. V., & Duque, P. (2013). On the physiological significance
769 of alternative splicing events in higher plants. *Protoplasma, 250*(3), 639-650.
770 doi: 10.1007/s00709-012-0448-9
771 Chen, Y., & Varani, G. (2013). Engineering RNA-binding proteins for biology. *FEBS*
772 *J, 280*(16), 3734-3754. doi: 10.1111/febs.12375
773 Cho, S., Hoang, A., Sinha, R., Zhong, X. Y., Fu, X. D., Krainer, A. R., & Ghosh, G.
774 (2011). Interaction between the RNA binding domains of Ser-Arg splicing
775 factor 1 and U1-70K snRNP protein determines early spliceosome assembly.
776 *Proc Natl Acad Sci U S A, 108*(20), 8233-8238. doi:
777 10.1073/pnas.1017700108
778 Clough, S. J., & Bent, A. F. (1998). Floral dip: a simplified method for Agrobacterium-
779 mediated transformation of Arabidopsis thaliana. *Plant J, 16*(6), 735-743.
780 Cooke, C., & Alwine, J. C. (2002). Characterization of specific protein-RNA
781 complexes associated with the coupling of polyadenylation and last-intron
782 removal. *Mol Cell Biol, 22*(13), 4579-4586.
783 Cooke, C., Hans, H., & Alwine, J. C. (1999). Utilization of splicing elements and
784 polyadenylation signal elements in the coupling of polyadenylation and last-
785 intron removal. *Mol Cell Biol, 19*(7), 4971-4979.
786 Ding, F., Cui, P., Wang, Z., Zhang, S., Ali, S., & Xiong, L. (2014). Genome-wide
787 analysis of alternative splicing of pre-mRNA under salt stress in Arabidopsis.
788 *Bmc Genomics, 15*, 431. doi: 10.1186/1471-2164-15-431
789 Drechsel, G., Kahles, A., Kesarwani, A. K., Stauffer, E., Behr, J., Drewe, P., Ratsch,
790 G., & Wachter, A. (2013). Nonsense-mediated decay of alternative precursor

791 mRNA splicing variants is a major determinant of the Arabidopsis steady state
792 transcriptome. *Plant Cell, 25*(10), 3726-3742. doi: 10.1105/tpc.113.115485
793 Durek, P., Schmidt, R., Heazlewood, J. L., Jones, A., MacLean, D., Nagel, A.,
794 Kersten, B., & Schulze, W. X. (2010). PhosPhAt: the Arabidopsis thaliana
795 phosphorylation site database. An update. *Nucleic Acids Res, 38*(Database
796 issue), D828-834. doi: 10.1093/nar/gkp810
797 Fortes, P., Bilbao-Cortes, D., Fornerod, M., Rigaut, G., Raymond, W., Seraphin, B., &
798 Mattaj, I. W. (1999a). Luc7p, a novel yeast U1 snRNP protein with a role in 5'
799 splice site recognition. *Genes Dev, 13*(18), 2425-2438.
800 Fortes, P., Kufel, J., Fornerod, M., Polycarpou-Schwarz, M., Lafontaine, D.,
801 Tollervey, D., & Mattaj, I. W. (1999b). Genetic and physical interactions
802 involving the yeast nuclear cap-binding complex. *Mol Cell Biol, 19*(10), 6543-
803 6553.
804 Fukumura, K., Taniguchi, I., Sakamoto, H., Ohno, M., & Inoue, K. (2009). U1-
805 independent pre-mRNA splicing contributes to the regulation of alternative
806 splicing. *Nucleic Acids Res, 37*(6), 1907-1914. doi: 10.1093/nar/gkp050
807 Gohring, J., Jacak, J., & Barta, A. (2014). Imaging of endogenous messenger RNA
808 splice variants in living cells reveals nuclear retention of transcripts
809 inaccessible to nonsense-mediated decay in Arabidopsis. *Plant Cell, 26*(2),
810 754-764. doi: 10.1105/tpc.113.118075
811 Golovkin, M., & Reddy, A. S. (1998). The plant U1 small nuclear ribonucleoprotein
812 particle 70K protein interacts with two novel serine/arginine-rich proteins. *Plant*
813 *Cell, 10*(10), 1637-1648.
814 Golovkin, M., & Reddy, A. S. (2003). Expression of U1 small nuclear
815 ribonucleoprotein 70K antisense transcript using APETALA3 promoter
816 suppresses the development of sepals and petals. *Plant Physiol, 132*(4),
817 1884-1891.
818 Gonatopoulos-Pournatzis, T., & Cowling, V. H. (2014). Cap-binding complex (CBC).
819 *Biochem J, 457*(2), 231-242. doi: 10.1042/BJ20131214
820 Gouy, M., Guindon, S., & Gascuel, O. (2010). SeaView version 4: A multiplatform
821 graphical user interface for sequence alignment and phylogenetic tree
822 building. *Mol Biol Evol, 27*(2), 221-224. doi: 10.1093/molbev/msp259

823 Guiro, J., & O'Reilly, D. (2015). Insights into the U1 small nuclear ribonucleoprotein
824 complex superfamily. *Wiley Interdisciplinary Reviews-Rna, 6*(1), 79-92. doi:
825 Doi 10.1002/Wrna.1257
826 Heazlewood, J. L., Durek, P., Hummel, J., Selbig, J., Weckwerth, W., Walther, D., &
827 Schulze, W. X. (2008). PhosPhAt: a database of phosphorylation sites in
828 Arabidopsis thaliana and a plant-specific phosphorylation site predictor.
829 *Nucleic Acids Res, 36*(Database issue), D1015-1021. doi:
830 10.1093/nar/gkm812
831 Heim, A., Grimm, C., Muller, U., Haussler, S., Mackeen, M. M., Merl, J., Hauck, S.
832 M., Kessler, B. M., Schofield, C. J., Wolf, A., & Bottger, A. (2014). Jumonji
833 domain containing protein 6 (Jmjd6) modulates splicing and specifically
834 interacts with arginine-serine-rich (RS) domains of SR- and SR-like proteins.
835 *Nucleic Acids Res, 42*(12), 7833-7850. doi: 10.1093/nar/gku488
836 Hernandez, H., Makarova, O. V., Makarov, E. M., Morgner, N., Muto, Y., Krummel, D.
837 P., & Robinson, C. V. (2009). Isoforms of U1-70k control subunit dynamics in
838 the human spliceosomal U1 snRNP. *PLoS One, 4*(9), e7202. doi:
839 10.1371/journal.pone.0007202
840 Hoffman, B. E., & Grabowski, P. J. (1992). U1 snRNP targets an essential splicing
841 factor, U2AF65, to the 3' splice site by a network of interactions spanning the
842 exon. *Genes Dev, 6*(12B), 2554-2568.
843 Hori, K., & Watanabe, Y. (2005). UPF3 suppresses aberrant spliced mRNA in
844 Arabidopsis. *Plant J, 43*(4), 530-540. doi: 10.1111/j.1365-313X.2005.02473.x
845 Kaida, D. (2016). The reciprocal regulation between splicing and 3'-end processing.
846 *Wiley Interdiscip Rev RNA, 7*(4), 499-511. doi: 10.1002/wrna.1348
847 Kaida, D., Berg, M. G., Younis, I., Kasim, M., Singh, L. N., Wan, L., & Dreyfuss, G.
848 (2010). U1 snRNP protects pre-mRNAs from premature cleavage and
849 polyadenylation. *Nature, 468*(7324), 664-668. doi: 10.1038/nature09479
850 Kalyna, M., Simpson, C. G., Syed, N. H., Lewandowska, D., Marquez, Y., Kusenda,
851 B., Marshall, J., Fuller, J., Cardle, L., McNicol, J., Dinh, H. Q., Barta, A., &
852 Brown, J. W. (2012). Alternative splicing and nonsense-mediated decay
853 modulate expression of important regulatory genes in Arabidopsis. *Nucleic*
854 *Acids Res, 40*(6), 2454-2469. doi: 10.1093/nar/gkr932
855 Kersey, P. J., Allen, J. E., Armean, I., Boddu, S., Bolt, B. J., Carvalho-Silva, D.,
856 Christensen, M., Davis, P., Falin, L. J., Grabmueller, C., Humphrey, J.,

857 Kerhornou, A., Khobova, J., Aranganathan, N. K., Langridge, N., Lowy, E.,
858 McDowall, M. D., Maheswari, U., Nuhn, M., Ong, C. K., Overduin, B., Paulini,
859 M., Pedro, H., Perry, E., Spudich, G., Tapanari, E., Walts, B., Williams, G.,
860 Tello-Ruiz, M., Stein, J., Wei, S., Ware, D., Bolser, D. M., Howe, K. L.,
861 Kulesha, E., Lawson, D., Maslen, G., & Staines, D. M. (2016). Ensembl
862 Genomes 2016: more genomes, more complexity. *Nucleic Acids Res, 44*(D1),
863 D574-580. doi: 10.1093/nar/gkv1209
864 Kervestin, S., & Jacobson, A. (2012). NMD: a multifaceted response to premature
865 translational termination. *Nat Rev Mol Cell Biol, 13*(11), 700-712. doi:
866 10.1038/nrm3454
867 Kim, D., Pertea, G., Trapnell, C., Pimentel, H., Kelley, R., & Salzberg, S. L. (2013).
868 TopHat2: accurate alignment of transcriptomes in the presence of insertions,
869 deletions and gene fusions. *Genome Biol, 14*(4), R36. doi: 10.1186/gb-2013-
870 14-4-r36
871 Knop, K., Stepien, A., Barciszewska-Pacak, M., Taube, M., Bielewicz, D., Michalak,
872 M., Borst, J. W., Jarmolowski, A., & Szweykowska-Kulinska, Z. (2016). Active
873 5' splice sites regulate the biogenesis efficiency of Arabidopsis microRNAs
874 derived from intron-containing genes. *Nucleic Acids Res*. doi:
875 10.1093/nar/gkw895
876 Koncz, C., Dejong, F., Villacorta, N., Szakonyi, D., & Koncz, Z. (2012). The
877 spliceosome-activating complex: molecular mechanisms underlying the
878 function of a pleiotropic regulator. *Front Plant Sci, 3*, 9. doi:
879 10.3389/fpls.2012.00009
880 Kornblihtt, A. R., Schor, I. E., Allo, M., Dujardin, G., Petrillo, E., & Munoz, M. J.
881 (2013). Alternative splicing: a pivotal step between eukaryotic transcription
882 and translation. *Nat Rev Mol Cell Biol, 14*(3), 153-165. doi: 10.1038/nrm3525
883 Laubinger, S., Sachsenberg, T., Zeller, G., Busch, W., Lohmann, J. U., Ratsch, G., &
884 Weigel, D. (2008). Dual roles of the nuclear cap-binding complex and
885 SERRATE in pre-mRNA splicing and microRNA processing in Arabidopsis
886 thaliana. *Proc Natl Acad Sci U S A, 105*(25), 8795-8800. doi:
887 10.1073/pnas.0802493105
888 Lewis, J. D., Izaurralde, E., Jarmolowski, A., McGuigan, C., & Mattaj, I. W. (1996). A
889 nuclear cap-binding complex facilitates association of U1 snRNP with the cap-

890 proximal 5' splice site. *Genes & Development, 10*(13), 1683-1698. doi:
891 10.1101/gad.10.13.1683
892 Liao, Y., Smyth, G. K., & Shi, W. (2013). The Subread aligner: fast, accurate and
893 scalable read mapping by seed-and-vote. *Nucleic Acids Res, 41*(10), e108.
894 doi: 10.1093/nar/gkt214
895 Muller-McNicoll, M., Botti, V., de Jesus Domingues, A. M., Brandl, H., Schwich, O.
896 D., Steiner, M. C., Curk, T., Poser, I., Zarnack, K., & Neugebauer, K. M.
897 (2016). SR proteins are NXF1 adaptors that link alternative RNA processing to
898 mRNA export. *Genes Dev, 30*(5), 553-566. doi: 10.1101/gad.276477.115
899 Nakagawa, T., Suzuki, T., Murata, S., Nakamura, S., Hino, T., Maeo, K., Tabata, R.,
900 Kawai, T., Tanaka, K., Niwa, Y., Watanabe, Y., Nakamura, K., Kimura, T., &
901 Ishiguro, S. (2007). Improved Gateway binary vectors: high-performance
902 vectors for creation of fusion constructs in transgenic analysis of plants. *Biosci*
903 *Biotechnol Biochem, 71*(8), 2095-2100. doi: 10.1271/bbb.70216
904 Naro, C., Jolly, A., Di Persio, S., Bielli, P., Setterblad, N., Alberdi, A. J., Vicini, E.,
905 Geremia, R., De la Grange, P., & Sette, C. (2017). An Orchestrated Intron
906 Retention Program in Meiosis Controls Timely Usage of Transcripts during
907 Germ Cell Differentiation. *Dev Cell, 41*(1), 82-93 e84. doi:
908 10.1016/j.devcel.2017.03.003
909 Nesic, D., & Maquat, L. E. (1994). Upstream introns influence the efficiency of final
910 intron removal and RNA 3'-end formation. *Genes Dev, 8*(3), 363-375.
911 Ohtani, M., & Sugiyama, M. (2005). Involvement of SRD2-mediated activation of
912 snRNA transcription in the control of cell proliferation competence in
913 Arabidopsis. *Plant J, 43*(4), 479-490. doi: 10.1111/j.1365-313X.2005.02469.x
914 Papp, I., Mur, L. A., Dalmadi, A., Dulai, S., & Koncz, C. (2004). A mutation in the Cap
915 Binding Protein 20 gene confers drought tolerance to Arabidopsis. *Plant Mol*
916 *Biol, 55*(5), 679-686. doi: 10.1007/s11103-004-1680-2
917 Pimentel, H., Parra, M., Gee, S. L., Mohandas, N., Pachter, L., & Conboy, J. G.
918 (2016). A dynamic intron retention program enriched in RNA processing genes
919 regulates gene expression during terminal erythropoiesis. *Nucleic Acids Res,*
920 *44*(2), 838-851. doi: 10.1093/nar/gkv1168
921 Prigge, M. J., & Wagner, D. R. (2001). The arabidopsis serrate gene encodes a zinc-
922 finger protein required for normal shoot development. *Plant Cell, 13*(6), 1263-
923 1279.

924 Puig, O., Bragado-Nilsson, E., Koski, T., & Seraphin, B. (2007). The U1 snRNP-
925 associated factor Luc7p affects 5' splice site selection in yeast and human.
926 *Nucleic Acids Res, 35*(17), 5874-5885. doi: 10.1093/nar/gkm505
927 Raczynska, K. D., Simpson, C. G., Ciesiolka, A., Szewc, L., Lewandowska, D.,
928 McNicol, J., Szweykowska-Kulinska, Z., Brown, J. W., & Jarmolowski, A.
929 (2010). Involvement of the nuclear cap-binding protein complex in alternative
930 splicing in Arabidopsis thaliana. *Nucleic Acids Res, 38*(1), 265-278. doi:
931 10.1093/nar/gkp869
932 Raczynska, K. D., Stepien, A., Kierzkowski, D., Kalak, M., Bajczyk, M., McNicol, J.,
933 Simpson, C. G., Szweykowska-Kulinska, Z., Brown, J. W., & Jarmolowski, A.
934 (2013). The SERRATE protein is involved in alternative splicing in Arabidopsis
935 thaliana. *Nucleic Acids Res*. doi: 10.1093/nar/gkt894
936 Reddy, A. S., Marquez, Y., Kalyna, M., & Barta, A. (2013). Complexity of the
937 alternative splicing landscape in plants. *Plant Cell, 25*(10), 3657-3683. doi:
938 10.1105/tpc.113.117523
939 Rigo, F., & Martinson, H. G. (2008). Functional coupling of last-intron splicing and 3'-
940 end processing to transcription in vitro: the poly(A) signal couples to splicing
941 before committing to cleavage. *Mol Cell Biol, 28*(2), 849-862. doi:
942 10.1128/mcb.01410-07
943 Rigo, F., & Martinson, H. G. (2009). Polyadenylation releases mRNA from RNA
944 polymerase II in a process that is licensed by splicing. *RNA, 15*(5), 823-836.
945 doi: 10.1261/rna.1409209
946 Rosel, T. D., Hung, L. H., Medenbach, J., Donde, K., Starke, S., Benes, V., Ratsch,
947 G., & Bindereif, A. (2011). RNA-Seq analysis in mutant zebrafish reveals role
948 of U1C protein in alternative splicing regulation. *EMBO J, 30*(10), 1965-1976.
949 doi: 10.1038/emboj.2011.106
950 Rowley, M. J., Bohmdorfer, G., & Wierzbicki, A. T. (2013). Analysis of long non-
951 coding RNAs produced by a specialized RNA polymerase in Arabidopsis
952 thaliana. *Methods, 63*(2), 160-169. doi: 10.1016/j.ymeth.2013.05.006
953 Roy, D., Bhanja Chowdhury, J., & Ghosh, S. (2013). Polypyrimidine tract binding
954 protein (PTB) associates with intronic and exonic domains to squelch nuclear
955 export of unspliced RNA. *FEBS Lett, 587*(23), 3802-3807. doi:
956 10.1016/j.febslet.2013.10.005

957 Schlaen, R. G., Mancini, E., Sanchez, S. E., Perez-Santangelo, S., Rugnone, M. L.,
958 Simpson, C. G., Brown, J. W., Zhang, X., Chernomoretz, A., & Yanovsky, M.
959 J. (2015). The spliceosome assembly factor GEMIN2 attenuates the effects of
960 temperature on alternative splicing and circadian rhythms. *Proc Natl Acad Sci*
961 *U S A, 112*(30), 9382-9387. doi: 10.1073/pnas.1504541112
962 Schwab, R., Speth, C., Laubinger, S., & Voinnet, O. (2013). Enhanced microRNA
963 accumulation through stemloop-adjacent introns. *EMBO Rep, 14*(7), 615-621.
964 doi: 10.1038/embor.2013.58
965 Shao, W., Kim, H. S., Cao, Y., Xu, Y. Z., & Query, C. C. (2012). A U1-U2 snRNP
966 interaction network during intron definition. *Mol Cell Biol, 32*(2), 470-478. doi:
967 10.1128/MCB.06234-11
968 Shaul, O. (2015). Unique Aspects of Plant Nonsense-Mediated mRNA Decay.
969 *Trends Plant Sci, 20*(11), 767-779. doi: 10.1016/j.tplants.2015.08.011
970 Shen, S., Park, J. W., Lu, Z. X., Lin, L., Henry, M. D., Wu, Y. N., Zhou, Q., & Xing, Y.
971 (2014). rMATS: robust and flexible detection of differential alternative splicing
972 from replicate RNA-Seq data. *Proc Natl Acad Sci U S A, 111*(51), E5593-
973 5601. doi: 10.1073/pnas.1419161111
974 Staiger, D., & Brown, J. W. (2013). Alternative splicing at the intersection of biological
975 timing, development, and stress responses. *Plant Cell, 25*(10), 3640-3656.
976 doi: 10.1105/tpc.113.113803
977 Stepien, A., Knop, K., Dolata, J., Taube, M., Bajczyk, M., Barciszewska-Pacak, M.,
978 Pacak, A., Jarmolowski, A., & Szweykowska-Kulinska, Z. (2017).
979 Posttranscriptional coordination of splicing and miRNA biogenesis in plants.
980 *Wiley Interdiscip Rev RNA, 8*(3). doi: 10.1002/wrna.1403
981 Sullivan, C., & Howard, P. L. (2016). The Diverse Requirements of ARS2 in nuclear
982 cap-binding complex-dependent RNA Processing. *Rna & Disease*. doi:
983 10.14800/rd.1376
984 Umezawa, T., Sugiyama, N., Takahashi, F., Anderson, J. C., Ishihama, Y., Peck, S.
985 C., & Shinozaki, K. (2013). Genetics and phosphoproteomics reveal a protein
986 phosphorylation network in the abscisic acid signaling pathway in Arabidopsis
987 thaliana. *Sci Signal, 6*(270), rs8. doi: 10.1126/scisignal.2003509
988 Wachter, A., Tunc-Ozdemir, M., Grove, B. C., Green, P. J., Shintani, D. K., &
989 Breaker, R. R. (2007). Riboswitch control of gene expression in plants by

990 splicing and alternative 3' end processing of mRNAs. *Plant Cell, 19*(11), 3437-
991 3450. doi: 10.1105/tpc.107.053645
992 Wahl, M. C., Will, C. L., & Luhrmann, R. (2009). The spliceosome: design principles
993 of a dynamic RNP machine. *Cell, 136*(4), 701-718. doi:
994 10.1016/j.cell.2009.02.009
995 Wang, B. B., & Brendel, V. (2004). The ASRG database: identification and survey of
996 Arabidopsis thaliana genes involved in pre-mRNA splicing. *Genome Biol,*
997 *5*(12), R102. doi: 10.1186/gb-2004-5-12-r102
998 Wang, C., Tian, Q., Hou, Z., Mucha, M., Aukerman, M., & Olsen, O. A. (2007). The
999 Arabidopsis thaliana AT PRP39-1 gene, encoding a tetratricopeptide repeat
1000 protein with similarity to the yeast pre-mRNA processing protein PRP39,
1001 affects flowering time. *Plant Cell Rep, 26*(8), 1357-1366. doi: 10.1007/s00299-
1002 007-0336-5
1003 Wang, P., Xue, L., Batelli, G., Lee, S., Hou, Y. J., Van Oosten, M. J., Zhang, H., Tao,
1004 W. A., & Zhu, J. K. (2013). Quantitative phosphoproteomics identifies SnRK2
1005 protein kinase substrates and reveals the effectors of abscisic acid action.
1006 *Proc Natl Acad Sci U S A, 110*(27), 11205-11210. doi:
1007 10.1073/pnas.1308974110
1008 Webby, C. J., Wolf, A., Gromak, N., Dreger, M., Kramer, H., Kessler, B., Nielsen, M.
1009 L., Schmitz, C., Butler, D. S., Yates, J. R., 3rd, Delahunty, C. M., Hahn, P.,
1010 Lengeling, A., Mann, M., Proudfoot, N. J., Schofield, C. J., & Bottger, A.
1011 (2009). Jmjd6 catalyses lysyl-hydroxylation of U2AF65, a protein associated
1012 with RNA splicing. *Science, 325*(5936), 90-93. doi: 10.1126/science.1175865
1013 Will, C. L., & Luhrmann, R. (2001). Spliceosomal UsnRNP biogenesis, structure and
1014 function. *Curr Opin Cell Biol, 13*(3), 290-301.
1015 Will, C. L., & Luhrmann, R. (2011). Spliceosome structure and function. *Cold Spring*
1016 *Harb Perspect Biol, 3*(7). doi: 10.1101/cshperspect.a003707
1017 Wong, J. J., Au, A. Y., Ritchie, W., & Rasko, J. E. (2016). Intron retention in mRNA:
1018 No longer nonsense: Known and putative roles of intron retention in normal
1019 and disease biology. *Bioessays, 38*(1), 41-49. doi: 10.1002/bies.201500117
1020 Xing, D., Wang, Y., Hamilton, M., Ben-Hur, A., & Reddy, A. S. (2015). Transcriptome-
1021 Wide Identification of RNA Targets of Arabidopsis SERINE/ARGININE-
1022 RICH45 Uncovers the Unexpected Roles of This RNA Binding Protein in RNA
1023 Processing. *Plant Cell*. doi: 10.1105/tpc.15.00641

1024 Yap, K., Lim, Z. Q., Khandelia, P., Friedman, B., & Makeyev, E. V. (2012).
1025 Coordinated regulation of neuronal mRNA steady-state levels through
1026 developmentally controlled intron retention. *Genes Dev, 26*(11), 1209-1223.
1027 doi: 10.1101/gad.188037.112
1028 Yoine, M., Ohto, M. A., Onai, K., Mita, S., & Nakamura, K. (2006). The lba1 mutation
1029 of UPF1 RNA helicase involved in nonsense-mediated mRNA decay causes
1030 pleiotropic phenotypic changes and altered sugar signalling in Arabidopsis.
1031 *Plant J, 47*(1), 49-62. doi: 10.1111/j.1365-313X.2006.02771.x
1032

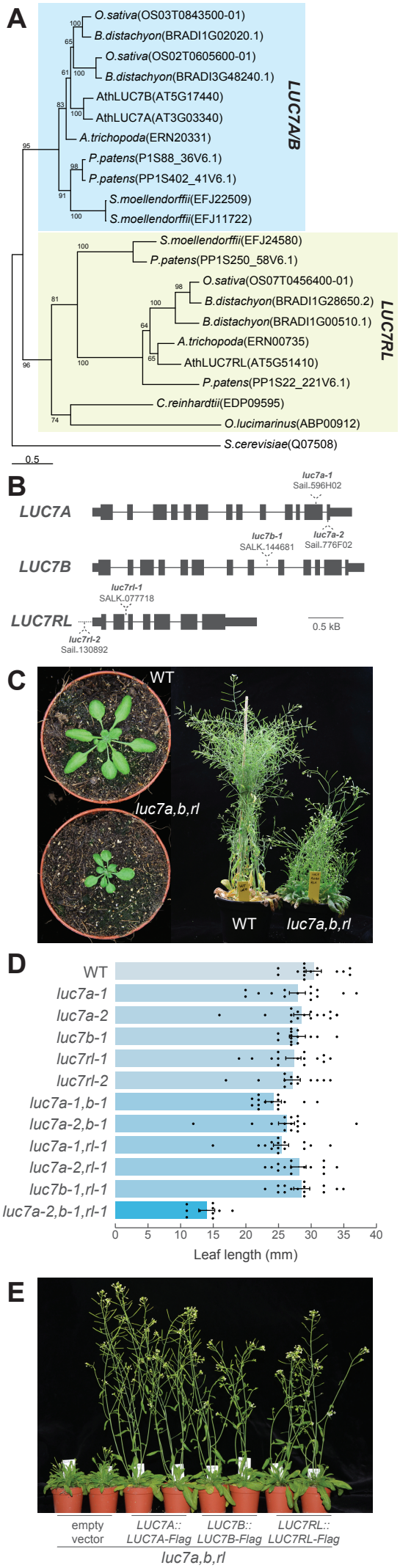
A
O.sativa(OS03T0843500-01)
B.distachyon(BRADI1G02020.1)
O.sativa(OS02T0605600-01)
B.distachyon(BRADI3G48240.1)
AthLUC7B(AT5G17440)
AthLUC7A(AT3G03340)
A.trichopoda(ERN20331)
P.patens(P1S88_36V6.1)
P.patens(PP1S402_41V6.1)
S.moellendorffii(EFJ22509)
S.moellendorffii(EFJ11722)
LUC7A/B
S.moellendorffii(EFJ24580)
P.patens(PP1S250_58V6.1)
O.sativa(OS07T0456400-01)
B.distachyon(BRADI1G28650.2)
B.distachyon(BRADI1G00510.1)
A.trichopoda(ERN00735)
AthLUC7RL(AT5G51410)
P.patens(PP1S22_221V6.1)
C.reinhardtii(EDP09595)
O.lucimarinus(ABP00912)
LUC7RL
S.cerevisiae(Q07508)
0.5
B
LUC7A
luc7a-1
Sail.596H02
LUC7B
luc7b-1
SALK_144681
luc7a-2
Sail.776F02
LUC7RL
luc7rl-1
SALK_077718
luc7rl-2
Sail.130892
0.5 kB
C
WT
luc7a,b,rl
WT
luc7a,b,rl
D
WT
luc7a-1
luc7a-2
luc7b-1
luc7rl-1
luc7rl-2
luc7a-1,b-1
luc7a-2,b-1
luc7a-1,rl-1
luc7a-2,rl-1
luc7b-1,rl-1
luc7a-2,b-1,rl-1
0 5 10 15 20 25 30 35 40
Leaf length (mm)
E
empty vector
LUC7A:: LUC7A-Flag
LUC7B:: LUC7B-Flag
LUC7RL:: LUC7RL-Flag
luc7a,b,rl

FIGURE 1

Figure 1: Arabidopsis LUC7 proteins redundantly control plant development

A: Phylogenetic analysis of LUC7 proteins in the plant kingdom using *Saccharomyces cerevisiae* as an external group.

B: Exon/intron structure of *Arabidopsis thaliana LUC7A*, *LUC7B* and *LUC7RL*. Dotted lines indicate the positions of T-DNA insertions.

C: WT and *luc7* triple mutant plants 21 days (left) and 45 days (right) after germination.

D: Length of the longest rosette leaf of 21 days-old WT, *luc7* single, double and triple mutant plants growing under long day conditions. Leaves of 10-15 individual plants were measured. Dots indicate individual data points. Error bars denote the SEM.

E: Complementation of *luc7a,b,rl* mutants by *LUC7A*, *LUC7B* and *LUC7RL* genomic rescue constructs. Transformation of an “empty” binary vector served as a control. Two independent transgenic lines for each construct are shown.

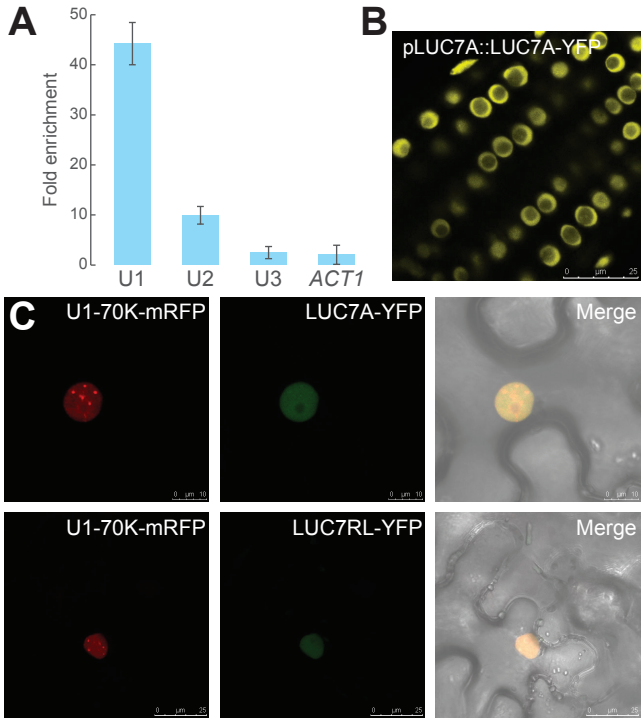

D

Identified protein	Aver. # of Peptides		Seq.Coverage (%)		MW (kDa)
	IP LUC7	IP WT	IP LUC7	IP WT	
LUC7A	45.75	0	71.9	0	47.4
U1 snRNP components					
U1-70k	5	0	13.3	0	50.4
SmB-a ; SmB-b	2.5	0	9.8	0	27.0
U1A	2	0	7.7	0	28.1
Splicing-related					
U2AF35A;U2AF35B	3.5	1	11.9	4.3	34.6
SCL30A;SCL33	2.75	0	12.3	0	20.2
SR45	1.75	0	5.2	0	44.6
RSZ21;RSZ22;RSZ22A	1.75	0	8.0	0	22.5
SR30	1	0	3.9	0	29.1
RS2Z33	1	0	2.9	0	32.9
SCL30	0.75	0	2.8	0	29.6
U2AF65A	0.75	0	1.7	0	60.7
RNA metabolism					
SERRATE	7.75	0	12.0	0	81.1
Cleavage factor AT4G25550	1.75	0	11.0	0	22.8
ABH1	1	0	1.4	0	96.6
Kinases					
SRPK4	8.5	0	16.2	0	59.4
AT4G25550	8.25	0	15.9	0	60.7
SRPK3	4.25	0	8.9	0	61.2

FIGURE 2

Figure 2: Arabidopsis LUC7 is an U1 snRNP component

A: RNA immunoprecipitation using a *pLUC7A:LUC7A-YFP, luc7a,b,rl* complemented line. Proteins were immunoprecipitated using GFP-specific affinity matrix and RNAs were extracted from the input and the immunoprecipitated. U1, U2, U3 snRNAs and *ACTIN* RNA were quantified using qRT-PCR. Enrichment of the respective RNA in LUC7A:LUC7A-YFP luc7a,b,rl transgenic lines was calculated over WT (negative control). Error bars denote the range of two biological replicates.

B: Subcellular localization of LUC7A in *pLUC7A:LUC7A-YFP luc7a,b,rl* in Arabidopsis transgenic plants. Roots of 9 day-old seedlings were analyzed using confocal microscopy. Scale bar indicates 25 µm.

C: U1-70K-mRFP and LUC7A-YFP or LUC7RL-YFP proteins were transiently expressed in *N. benthamiana*. The subcellular localization of mRFP and YFP fusion proteins was analyzed using confocal microscopy. Scale bars indicate 10 µm and 25 µm for upper and lower panel, respectively.

D: List of some LUC7-associated proteins identified by MS.

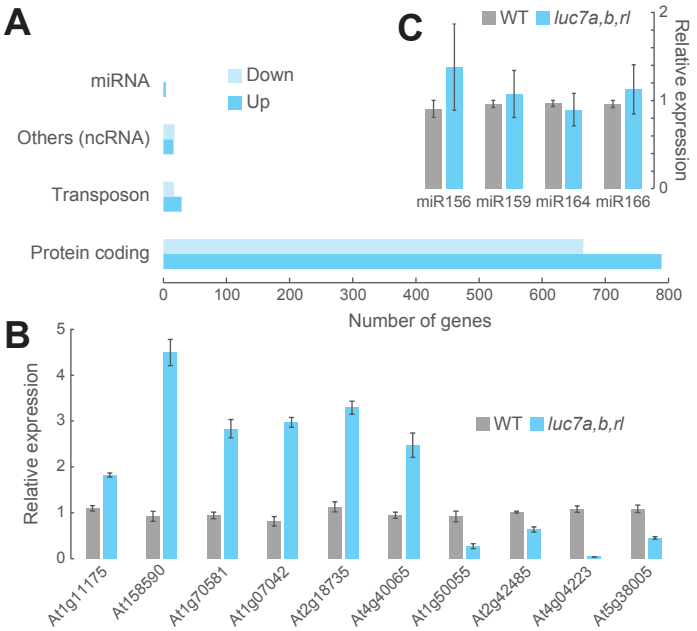

FIGURE 3

Figure 3: Mutations in *LUC7* results in misexpression of protein-coding and non-coding genes, but not in MIRNA genes

A: Differentially expressed genes in *luc7a,b,rl* mutant compared to WT.

B,C: qRT-PCR analysis of selected ncRNA (B) and miRNAs (C) in WT and *luc7a,b,rl.*
Error bars denote the SEM (n=3).

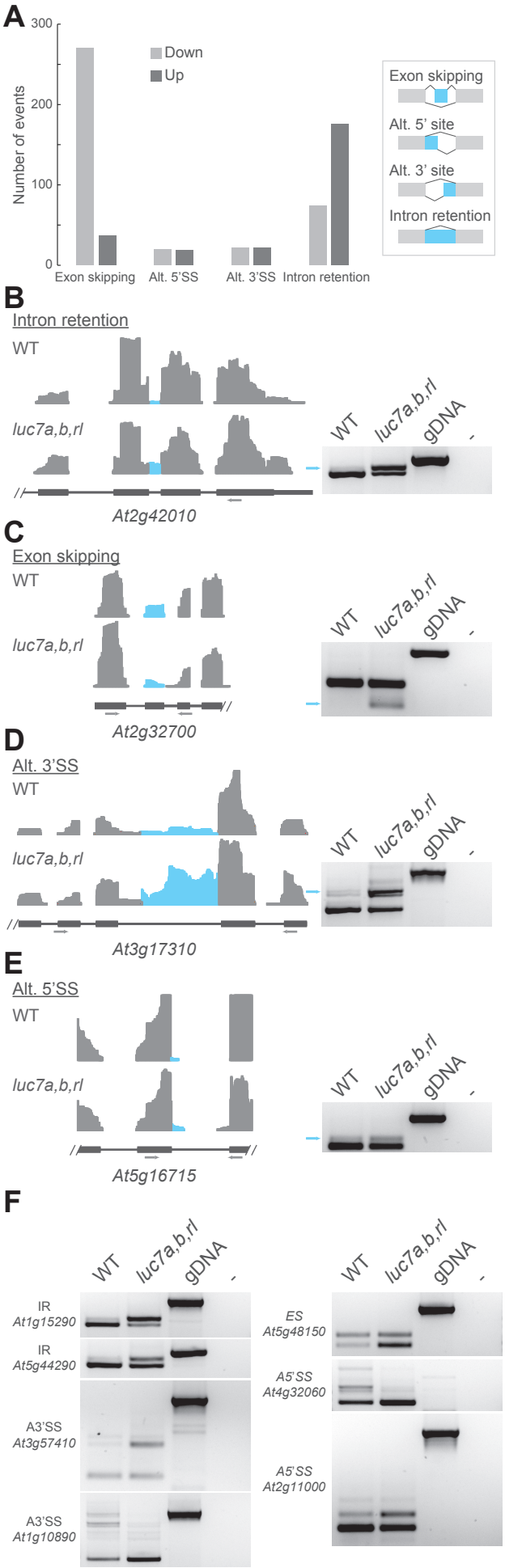
A
Number of events
300
200
100
0
Down
Up
Exon skipping
Alt. 5'SS
Alt. 3'SS
Intron retention
Exon skipping
Alt. 5' site
Alt. 3' site
Intron retention
B
Intron retention
WT
luc7a,b,rl
At2g42010
WT
luc7a,b,rl
gDNA
C
Exon skipping
WT
luc7a,b,rl
At2g32700
WT
luc7a,b,rl
gDNA
D
Alt. 3'SS
WT
luc7a,b,rl
At3g17310
WT
luc7a,b,rl
gDNA
E
Alt. 5'SS
WT
luc7a,b,rl
At5g16715
WT
luc7a,b,rl
gDNA
F
WT
luc7a,b,rl
gDNA
IR
At1g15290
IR
At5g44290
A3'SS
At3g57410
A3'SS
At1g10890
ES
At5g48150
A5'SS
At4g32060
A5'SS
At2g11000

FIGURE 4

Figure 4: Global analysis of splicing defects in *luc7* triple mutant.

A: Classification of splicing events changes in *luc7* triple mutant compared to WT.

B-F: Coverage plots and RT-PCR validation experiments for selected splicing events in WT and *luc7* triple mutant. Genomic DNA (gDNA) or water (-) served as a control. Primers positions are indicated with gray arrows. IR, intron retention; ES, exon skipping; Alt.3'SS, alternative 3'splicing site; Alt.5'SS, alternative 5'splicing site.

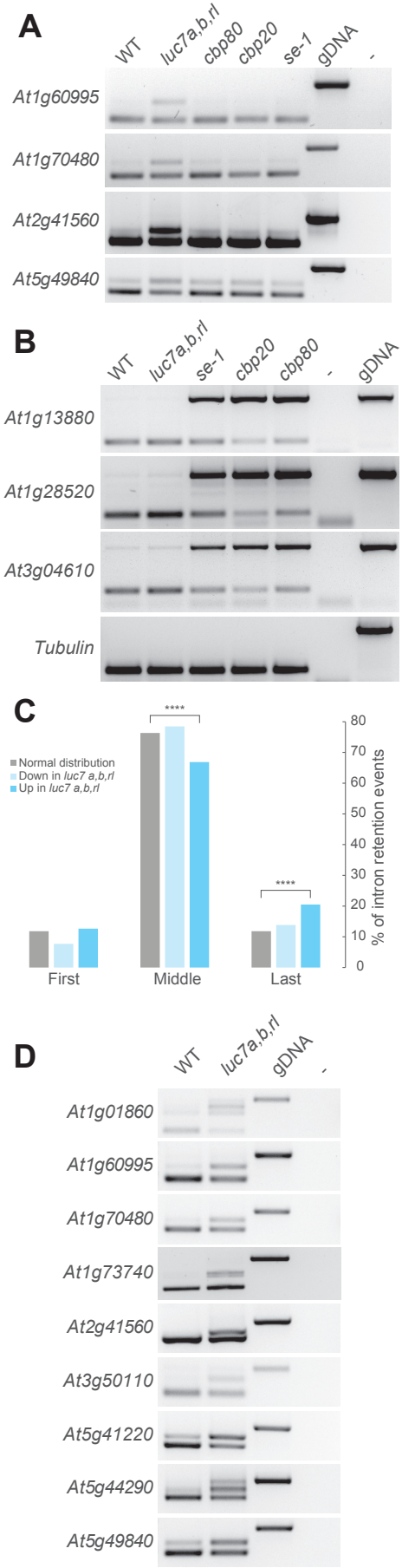

FIGURE 5

Figure 5: LUC7 proteins have a pronounced effect on terminal intron splicing

A: RT-PCR analysis of LUC7-dependent introns in WT, *luc7* triple mutant, *cbp80*, *cbp20* and *se-1* mutants.
B: RT-PCR analysis of CBC/SE-dependent introns in WT, *luc7* triple mutant, *cbp80*, *cbp20* and *se-1* mutants.
C: Classification of intron retention according to the intron position (first, middle, or last). Only genes with 3 or more introns were considered for this analysis. Terminal introns are significantly enriched among introns retained in *luc7* triple mutants (Fischer test; two-side $p < 0.0016$).
D: RT-PCR analysis of genes carrying retained terminal introns in WT and *luc7* triple mutants.

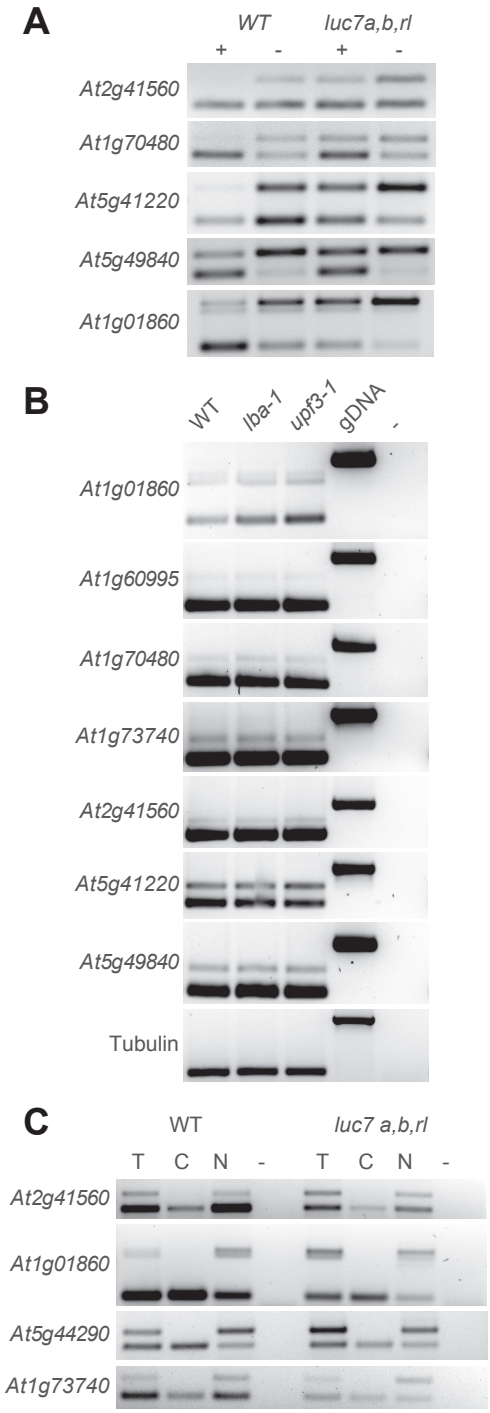

FIGURE 6

Figure 6: mRNAs containing retained LUC7-dependent terminal introns are NMD-insensitive and remain nuclear.

A: Splicing patterns of mRNAs carrying LUC7-dependent terminal introns in poly(A)+ and poly(A)- fractions.

B: RT-PCR analysis of LUC7-dependent terminal introns in WT and NMD mutants (*lba1* and *upf3-1*).

C: Splicing patterns of mRNAs isolated from total (T), cytosolic (C) and nuclear (N) fractions.

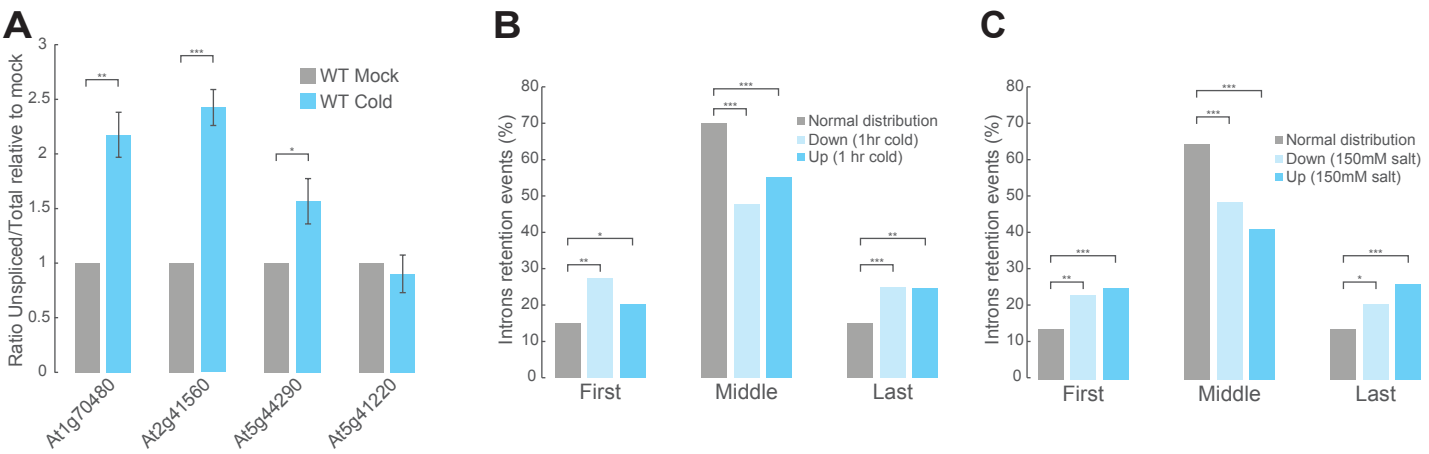

FIGURE 7

Figure 7: Splicing of LUC7 dependent terminal introns can be modulated by stress.

A: Seven days old WT seedlings were exposed to cold for 60 min. Splicing ratios (unspliced/total RNA) of four genes featuring a LUC7-dependent terminal intron were analyzed by qPCR. T-test was performed before calculating the relative to WT (* p=0,0208, ** p =0,0095, *** p = 0.004).

B-C: Classification of intron retention events in cold- (B) and salt-treated plants (C) The relative amount of retained/removed first, middle, and last intron in stress samples was compared to the relative amount of first, middle, and last intron among all expressed genes (normal distribution). Only genes with 3 or more introns were considered for this analysis.
* $p < 0.05$, ** $p < 0.01$, *** $p < 0.001$, **** $p < 0.0001$